Green Chemistry

PAPER

View Article Online
View Journal | View Issue



Cite this: *Green Chem.*, 2024, **26**, 6532

# Prospective hazard and toxicity screening of sodium-ion battery cathode materials†

Manuel Baumann, *[a] Jens F. Peters,[b] Marcel Häringer,[c] Marius Schmidt,[c] Luca Schneider,[c] Werner Bauer,[c] Joachim R. Binder[c] and Marcel Weil[a,d]

Sodium-ion batteries (SiBs) are considered as a serious alternative to the current lithium-ion batteries (LiBs). However, SiBs are an emerging technology in the early stage of development with a wide set of potential cathode material candidates available. Therefore, a major challenge is to identify the most promising and sustainable cathode materials for further research and potential commercialization, simultaneously considering relevant regulations such as the recent new EU Battery Regulation and Europe's chemicals strategy. Herein, we provide a comprehensive hazard and toxicity screening of promising SIB cathode material, which includes three different toxicity and hazard perspectives: (i) hazard traffic lights (HTL), (ii) total hazard points (THP), and (iii) human toxicity potential (HTox). Over 20 different SiB cathode compositions were screened together with three state-of-the-art LiB-cathodes for comparison. Inputs such as gravimetric energy density and required precursors were based on a comprehensive literature review, laboratory data, and calculations. All cathode active materials were analysed *via* a bottom-up approach. The results clearly showed that the energy density is one of the most important factors determining the choice of materials for SiBs and their corresponding related impacts. This screening can support a preliminary assessment of cathodes and help substitute selected precursors if they are associated with increased toxic hazards, therefore contributing to the ongoing discussions on more sustainable batteries and their labelling.

Received 22nd December 2023,
Accepted 15th April 2024

DOI: 10.1039/d3gc05098j

rsc.li/greenchem



## Introduction

Battery storage is considered as a main pillar to guarantee a safe, flexible and cost-effective energy and mobility transition towards renewables. This translates into significant market growth, with an expected global cumulative capacity of 504 GW to 1432 GW h by 2030.[1] Consequently, it is crucial to ensure the sustainable development of battery storage systems, considering their raw material extraction, purification, and manufacturing and design, for their transport, use and end-of-life management. This also includes the restriction of hazardous substances in batteries to minimize potential threats to the environment and human health. Accordingly, batteries have to be labelled regarding the amount of hazardous substances present (beside mercury, lead, and cadmium as restricted substances) under the new EU Battery Regulation.[2,3] Also, the EU's chemicals strategy for sustainability towards a toxic-free environment plays an important role to guarantee Europe's capability to motivation a safe and sustainable-by-design approach to chemicals, in particular those used in batteries. Thus, to achieve this, advanced tools, methods and models, data analysis capacities and early warning and action systems for chemicals have to be developed. This also entails the development of corresponding indicators and innovative risk assessment tools,[4] which is targeted on an international level by the OECD[5] and other ongoing discussions, *e.g.*, towards green and just chemistry.[6]

Sodium-ion batteries (SIBs) are considered one of the most promising alternatives to current lithium-ion batteries (LiBs) by avoiding several drawbacks related to sustainability, such as usage of critical raw materials, resource depletion, carbon footprint, material cost, safety, and toxicity.[7,8] Additionally, SIBs are considered drop-in technology for LIBs, allowing the use of comparable manufacturing steps. Thus, significant growth is expected for SIBs, with an increase in market demand from 135 GW h in 2019 to 270 GW h by 2025 (+671%).[9] There are several start-ups, and also established companies entering the market with different types of SIB chemistries.[10–13] SIB share

[a]*Institute for Technology Assessment and Systems Analysis, KIT – ITAS, Karlsruhe, Germany. E-mail: manuel.baumann@kit.edu*
[b]*University of Alcalá (UAH), Department of Economics, Alcalá de Henares, Madrid, Spain*
[c]*Institute for Applied Materials – Energy Storage Systems, KIT – IAM-ESS, Karlsruhe, Germany*
[d]*Helmholtz-Institute for Electrochemical Energy Storage, KIT – HIU, Ulm, Germany*
† Electronic supplementary information (ESI) available. See DOI: https://doi.org/10.1039/d3gc05098j

the same electrochemical principles as LiB, where their only difference is the use of sodium instead of lithium as the cathode and the electrolyte, respectively. Furthermore, for SIB aluminium is used as the current collector and hard carbon instead of (natural and synthetic) graphite as the anode.[14] In this case, the broadest field of research is currently cathode active materials (CAM), where a large number of different materials is being tested at a lower technology readiness level (TRL).[8,15,16] These materials can roughly be classified into two different types, *i.e.*, layered oxides and polyanionic materials. Additionally, the literature often provides a further, third classification for Prussian blue analogues (PBA). Here, the latter is a member of the family of polyanionic materials. More details on the structure and properties of these two types of CAM are provided in a previous work, and therefore not further discussed here in detail.[8]

Given that the cathode is one of the components that has a particularly high impact on the cost and environmental performance of an SIB cell,[7,8] it is necessary to screen a large number of different material combinations for SIB to determine their impacts on the environment and human health and the use of hazardous substances to guarantee a sustainable-by-design approach to chemicals for this type of battery. In this case, although a detailed screening of a large set of different cathode active materials (CAM) for SIB regarding their cost, criticality and carbon footprint is available in a recent work,[8] there is still a lack of methodologies for the early-stage screening of the hazards and toxicity aspects of CAM and their related precursors. This is of particular relevance considering the requirements stated in the EU chemicals strategy for sustainability towards a toxic-free environment, the OECD guidance for the identification and selection of safer chemicals and the requirements for battery labeling as defined in the new EU battery regulation.[2–5]

The goal of this work was to identify hazards and toxicity hotspots within a sustainable-by-design approach considering current regulations for emerging SIB CAM using a set of different complementary methods. For this purpose, a hazard screening approach based on (i) hazard traffic lights (HTL) and (ii) total hazard points (THP) was used. Both are based on information on potential hazards declared for chemical products according to the REACH regulation and the Seveso Directive[17–21] (which is also directly addressed in the Battery Passport Content Guidance[3]), and are contrasted with a life cycle assessment (LCA) approach using the Environmental Footprint method impact recommended by the EU[2,22] for categories devoted to human toxicity. In addition, representative LIB chemistries, namely lithium iron phosphate (LFP) and lithium nickel manganese cobalt oxide (NMC) batteries are included for comparison. A comparison of all the considered CAM was carried out in a qualitative way, by providing a score of risk to each cathode type and a indicative ranking as well as composite indicator based on THP and the HTox impact category obtained from the LCA. However, the results are not intended to directly benchmark different chemistries, but rather contribute to the development and discussion of demanded but missing innovative risk assessment tools for chemicals and related hazards in the field of emerging batteries, using SiB as an example.[4]

## Literature review

There is an increasing demand for the assessment and guidance on the use of less toxic and safer materials for battery development.[2,4,5] In this section, an overview of the available literature on the early screening of chemicals for emerging battery systems is provided. Here, the scope is beyond SIB, given that there is very little literature available explicitly targeting SIB. This enabled us to include relevant methods as well as studies that deal with hazards and toxicity issues for batteries. The review was carried out using Google Scholar, Wiley and Science Direct, with the oldest publication dating back to 2016.

Hazards in the sense of the EU Regulation on classification, labelling and packaging of substances and mixtures,[23] such as explosion or toxicity, can appear over the entire life cycle of batteries, starting from their material extraction, production, use, and end of life (recycling), and vary with battery chemistry and performance. Here, at any of the life cycle stages, the wrong treatment of chemicals or accidents may lead to severe impacts on the environment and human health.[21,24] However, it is difficult to identify potentials hazards in early technology development stages (or technology readiness levels – TRL) due to two aspects, as follows: (i) there is no common standard for these assessment methods[4] and (ii) there is often no sufficient data available for a robust assessment of new chemicals. Additionally, there may be a high number of potential material combinations that have to be screened but for which data are only available on a lab-scale level. This would require processes to be upscaled to obtain meaningful comparisons with state-of-the-art technologies that already benefited from a longer development and market diffusion process (including scale and experience curves). Therefore, instead of using detailed assessments such as life-cycle assessments (LCA), which require thorough modelling of all process chains, a rather simplified screening of electrode materials or precursors is more appropriate at the early TRL[25] to enable a sustainable-by-design approach from the beginning of technology development. This allows a quick and agile assessment supporting the selection of materials under sustainability aspects and minimizes hazards. These criteria and models should be flexible, modular, and easy to communicate if, *e.g.*, new material candidates are tested. After this first screening is presented, the promising materials will be subjected to a detailed sustainability assessment.[26]

As indicated in Table 1, only a few studies exist that provide easy indicators for low TRL battery technology and allow a direct comparison with acceptable uncertainty levels. In addition, there is no study that provides a comprehensive overview of potential hazards related to SIB. Thus, as stated before, this review is extended towards other emerging battery chem-

**Table 1** Overview of available screening studies for early-stage material screening for emerging electrochemical energy storage

| Source | Technology | Method | Indicators | Comment |
|---|---|---|---|---|
| Peters *et al.*[27] | One SIB-chemistry (layered oxide with Ni, Mn) compared to LIB chemistries form different studies | Life cycle assessment cut-off system model is used according to ecoinvent 3.2, ReCiPe midpoint method. | Fossil depletion potential (FDP), global warming potential (GWP), terrestrial acidification potential (TAP), human toxicity potential (HTP), and freshwater and marine eutrophication (FEP and MEP) 1 kW h of storage capacity. | Na-ion batteries are found to be promising regarding the used impact categories, in particular HTP, where SIB have the lowest impact. |
| Peters *et al.*[7] | 5 different SIB-Chemistries, compared to 2 state-of-the-art LiB technologies | Life cycle assessment based on own generic cell model cut-off system model is used according to ecoinvent 3.6, ILCD impact categories. | Human toxicity potential in mCTU per kW h, considering cancer and non-cancer effects based on USEtox 1 kW h of storage capacity. | Highest impacts result, depending on the chemistry from active cathode materials. |
| Rey *et al.*[29] | $Na_3V_2(PO_4)_3$ with ten different cathodes (*e.g.*, hierarchical carbon-NVP", "rGO-LbL NVP) | Life cycle assessment, using several ReCiPe 2016 Midpoint (H) indicators. | 18 indicators, focus on global warming potential, but human and ecotoxicity considered, per 1 kg and one kW h of cathode considering laboratory-scale approaches. | All the cathodes have certain levels of toxicity. In particular processes, where the generated wastewater strongly contributes to toxicity estimations. |
| Ellingsen *et al.*[25,31] based on ref. 18 | $AlCl_3$/EMIMCl ionic liquid electrolyte | Use of a set of LCA-based indicators and others based on LiSET method. | Material efficiency (specific energy, power density, synthesis material losses), environmental intensity of materials (exposure risks and hazards, supply risk, damage to human health, damage to ecosystems, climate change potential, recyclability, cycle lifetime) and energy efficiency. | 12 candidate electrode materials are analysed, each alternative has a drawback on some selected indicators. |
| Gschwind *et al.*[26] | Fluoride-ion cell cathode and anode materials | Use of CLP regulations, hazard statements and total hazard points, hazard traffic lights as qualitative indicator, total hazard points using lower tier values to quantify potential hazards and *via* LCA where possible. | Theoretical cell performance, hazard traffic lights as qualitative indicator, total hazard points using lower tier values to quantify potential hazards of 1 kW h of storage capacity. | F-ion and metallic ion precursor are analysed, $BiF_3$ and $AlF_3$ as the safest variant, whereas $ZnF_2$ is the most dangerous cathode material. The assessment *via* LCA is discussed theoretically and showed that most precursors are not available in USEtox. |
| Gschwind *et al.*[32] | Chloride ion battery, anode, cathode, and electrolyte candidates. | Use of CLP regulations, hazard statements and total hazard points, hazard traffic lights as qualitative indicator, total hazard points using lower tier values to quantify potential hazards. | Gravimetric as well as volumetric energy density, hazard traffic lights as qualitative indicator, total hazard points using lower tier values to quantify potential hazards of 1 kW h of storage capacity. | Use of REACH and CLP regulations for qualitative screening. |
| Rodriguez *et al.* (2016)[20] | Different battery types, including, lead acid, LiB (LiNMC, LiLFP, NCA), Redox Flow (V–V, Ce–Fe) Other (Zn–Air, NaS) | Use of CLP regulations, hazard statements and total hazard points, hazard traffic lights as qualitative indicator, total hazard points using lower tier values to quantify potential hazards. | Hazard traffic lights as qualitative indicator, total hazard points using lower tier values to quantify potential hazards of 1 kW h of storage capacity. | The results serve as an example for the application of the method. All analyzed technologies pose some hazards with very different magnitudes. |
| He *et al.* (2022)[33] | LiLFP, LiNMC and lithium manganese oxide (NMO), and three redox flow batteries (vanadium redox, zinc-bromine, and all-iron). | Use of an established chemical hazard assessment (CHA) framework (GreenScreen® for Safer Chemicals). Results are combined into a single score, for several materials, *via* the use of stochastic multicriteria acceptability analysis (SMAA). | Harmonized and aggregated to single-value hazard scores in total 20 endpoints with a hazard score sorted into six different toxicity groups, *e.g.*, carcinogenic, and mutagenic toxicity, reproductive, developmental and endocrine toxicity and physical hazards of 1 kW h of storage capacity. | Almost all materials from the selected battery types, including reagents and intermediates, inherently exhibit high hazard. There is a need to identity a clear alternative. |

istries to gather relevant indicators and related methods for screening of active materials.

Life cycle assessment approaches are already used to analyze hazards such as human and environmental toxicity, as in the case by Peters *et al.*,[27] where one SIB was compared with different LIB chemistries from several sources. In another work, five different SIB and two LIB chemistries were analyzed with an updated dataset adopting a BatPaC model.[7,28] Another study focused on SIB, in particular $Na_3V_2(PO_4)_3$,[29] where 10 different variants of the same cathode were also analyzed. Here, the authors mainly evaluated the global warming potential, but the impact category human toxicity was included for the detailed assessment. LCA was also used in a more general approach in the case of[30] for nanoscale cathode materials for lithium-ion batteries. A more general LCA framework (LiSET) is provided by Hung *et al.*[25] Here, a traffic light color grading system was used to account for the high uncertainty of analysis at the early-stage analysis considering numerous environmental aspects and hazards assessed. The LiSET method was used later by Ellingsen *et al.*[31] for the evaluation of aluminum batteries with an $AlCl_3$/EMIMCl ionic liquid electrolyte. However, all the LCA-based approaches focus on potential toxic impacts along the manufacturing chain, and not on the toxicity of the materials themselves, as targeted by REACH and the EU battery regulation. Works that focus on the potential hazards of the materials themselves that are contained in batteries or required for their manufacturing are comparably scarce. One example is the work by Gschwind *et al.*,[26] where an explorative toxicity screening was presented for seven cathode and nine anode variations for fluoride ion batteries. A comparable work from the same team of authors based on theoretical volumetric and gravimetric densities was carried out for chloride ion batteries using safety and toxicity for evaluation.[32] In both cases, REACH[17] and CLP regulations[23] were used for toxicity screening of nine cathode and eight anode materials. The method was based on the use of the so-called hazard traffic lights, which has also been applied for other state-of-the-art technologies such as LiB and redox flow batteries.[20] He *et al.* carried out a comparable work also analyzing different LIB and vanadium redox flow battery chemistries using a chemical hazard assessment *via* GreenScreen.[33] Subsequently, the results were combined into a single score using stochastic multicriteria decision analysis.

It can be seen that a wide variety of methods is used to conduct early-stage screenings of potential hazards of materials used for battery development. LCA is the most established and most frequently used approach but has a focus that is different from the scope of the EU Battery Regulation, which targets the content of hazardous materials within the battery. In this case, approaches that are more in line with the latter are the hazard traffic lights and total hazard points. In the study by Gschwind *et al.*,[26,32] both methods were used but in a rather qualitative way. A general framework to design safe and sustainable by design criteria for chemicals and materials based on current European legislation is provided in the EU's 'safe and sustainable by design' framework,[34] where hazard assessments represent the first step within a comprehensive approach entailing several methodologies and criteria. However, there is a lack of literature enabling the requirements towards hazard labelling within the battery regulation and the Battery Passport to be addressed in a prospective proactive way. Within this work, the THP and HTP methods are updated and applied together with an LCA-oriented toxicity assessment for evaluating their applicability in the early-stage screening of battery materials considering recent and future regulatory requirements.

## Methodology

Our approach extends the framework for the early-stage screening of CAM in terms of cost, criticality and carbon footprint developed in a previous work.[8] The focus was specifically toxicity and material hazards, applying three different approaches, as follows: (i) hazard traffic lights (HTL), (ii) total hazard points (THP) and (iii) human toxicity indicator of life cycle assessment (LCA), as indicated in Fig. 1. The two former methods are based on information on potential hazards, which was available in the registration, evaluation, authorization and restriction of chemicals (REACH) regulation[17] and the Seveso Directive,[18] developing and updating the method suggested by Rodriguez-García *et al.*[20] REACH serves as a base for the restriction of chemicals, which has recently gained some attention due to the discussion of banning per- and polyfluoroalkyl substances (PFAS),[35] which are also part of electrolyte, binders, and separators for LiB and SiB, but not considered in this analysis given that our focus was on CAM. Three simple composite indicators (human toxicity, total hazard points and hazard traffic lights) are used within this approach, which complement each other given that they cover very different aspects, as explained in Section 2. As shown in Fig. 1, the first step is based on a comprehensive literature review for different CAM and to derive the mass shares and properties of different materials (here indicated with $m_a$ and $m_c$, respectively) and the precursors used for the same ($m_{a1}$, $m_{c1}$...).

Then, the synthesis steps are summarized, and the precursor data extracted for the assessment to the extent provided by the underlying works. For all materials required for CAM synthesis, the corresponding CAS numbers are obtained and linked with the specific hazard statements as contained in the ECHA database or the toxicity impacts obtained from the ecoinvent database. Subsequently, the results are aggregated for each CAM, obtaining a picture of toxicity hotspots. Finally, a qualitative comparison of the different LIB and SIB CAM is carried out *via* a simple rescaling and weighted sum approach.

### Assessed SIB chemistries and specific energy

In total, 24 different SIB CAM were screened and compared with three LIB state-of-the-art technologies, namely LFP, NMC111 and NMC622, representing current battery technologies. The selection of the materials subjected to screening is

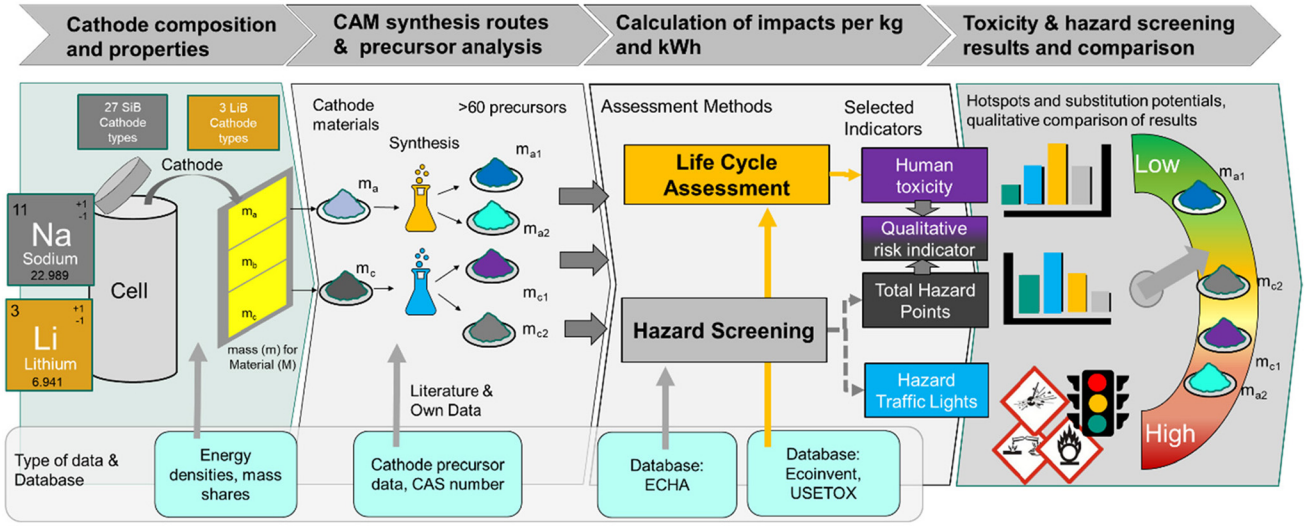


**Fig. 1** Overall methodology for the hazard screening of SIB; the benchmarking and the scope of the study.

based on an exhaustive literature review and expert judgement, aiming to provide a base for further assessments in this field. Correspondingly, not all possible material combinations are covered here, such as varying iron phosphate stoichiometries or Prussian White variations.[36–40]

In the case of the cathodes considered here, all required precursors were extracted from the corresponding publications to trace the used precursors and the corresponding synthesis routes, as depicted in Table 2. Accordingly, a large number of different chemical substances is analyzed (in total 63). It is worth mentioning that most of the used literature is based on lab-scale processes, given that most materials are not produced on a bulk level nowadays. Therefore, the corresponding synthesis routes, if available, may vary for the large-scale production of the analyzed materials. The specific capacity of the different cathode materials was derived from their average potential without a counter electrode.[8] In the case that not all ions are intercalated in the CAM, the theoretical capacity may not be representative, and thus the specific energy is derived from literature. When no information on the reversible capacity or the average potential is available, the integral of the potential-capacity curve was used.[8] In the case of $NaV_2(PO_4)$ and $Na_2MnPO_4F$, several synthesis routes using different precursors were analyzed, which are correspondingly presented in Table 1. It must be mentioned that the solvents were not analyzed given that they are considered to be recovered, and in some cases, it was not traceable which type of solvent was used. Instead, they are mentioned additionally in the results section based on the synthesized CAM where possible in the SI.

### Hazard traffic lights

The hazard traffic light method (HTL) is a qualitative visual way to quickly identify potential hazards and builds on the European Parliament on classification, labelling, and packaging (CPL),[23] which itself stems from the United Nations' Globally Harmonized System (GHS).[72] In terms of reporting, the Battery Regulation has to complement these regulations and corresponding hazard classes.[3] The hazard statements are based on[23] and refer to different classes, including physical (flammable, explosive...), health (acute toxicity, carcinogenic...) and environmental (hazardous to aquatic environment) hazards. Specifically, simple color codes for material hazards were used based on the signal words danger (yellow), warning (red) and no hazard (gray). The HTL does not include green signs, given that this may be understood as "non-toxic" or "non-hazardous", which at the end will be inconsistent with the regulation. Each hazard statement has a code of the form H*xxx* (where *xxx* are three numbers), with 62 statements, which are grouped into 28 hazard classes, as indicated in Fig. 2. Additionally, the nine so-called REACH-CLP pictograms/hazard symbols used for hazardous substance labelling are included in Fig. 2. More details on the HTP method can be found in.[20] It is recommended to use the harmonized classification tables under CLP within the EU battery regulation and to carry out a self-classification if some substances are missing,[3] which is very probable, as explained in the following.

In the case of the HTL, the first step is to identify the hazards allocated to a certain substance. This can be done by simply using the manufacturers' product sheets and the related hazard statement and warning. Alternatively, the webpage of the European chemistry association (ECHA)[73] *via* the database for information on substances of concern (SCIP)[74] can be used. SCIP provides over 7 million searchable article notifications and is recommended as source for chemical screening activities[5] and is also recommended in the frame of the battery passport.[3] Then, the identified substances are visualized in a graph or table in corresponding colors based on the stated hazards (*e.g.*, danger warning and no hazard

 

Table 2 Overview of analyzed SIB chemistries and corresponding precursors and synthesis routes, energy densities, energy densities taken from[8]

| Material | Synthesis routes | Reversible specific energy W h $kg^{-1}$ | Source |
|---|---|---|---|
| Lithium-ion batteries | | | |
| NMC111 | Synthesis: solution of $CoSO_4$·$NiSO_4$ and $MnSO_4$I in $H_2O$@60 °C/100 °C. $NH_4OH$ + NaOH added. Mixed with $Li_2CO_3$ and heated at 850 °C for 6 h in air. | 592 | 41 and 42 |
| NMC622 | Synthesis: solution of $CoSO_4$·$NiSO_4$ and $MnSO_4$I in $H_2O$@60 °C/100 °C. $NH_4OH$ + NaOH added. Mixed with $Li_2CO_3$ and heated at 850 °C for 6 h in air. | 629 | 42 |
| LFP | FeSO4·7$H_2O$ and 6 mmol H3$PO_4$ 16.2 mmol LiOH·$H_2O$ were dissolved in glycol, with constant stirring for five minutes. Then the mixture was inserted into a 40 mL autoclave and heated at 180 °C for 10 h, with $LiFePO_4$ nanoplates being formed at the bottom. The precipitate was washed with water and ethanol before drying at 60 °C for 6 h. | 569 | 43 |
| **Sodium ion batteries** | | | |
| $Na_3V_2(PO_4)_3$ | Synthesis 1: dissolve sodium acetate, vanadium acetylacetonate and phosphoric acid in tetraethylene glycol. Add flammable liquid diluent (not specified which one) and ignite liquid on hot plate at 470 °C. Powder obtained after heating at 800 °C for 5 h. | 381 | 44 |
| | Synthesis 2: dissolve sodium carbonate and ammonium dihydrogen phosphate in distilled water (solution A). Dissolve vanadium acetylacetonate in ethanol (solution B). Drop solution A into B. Evaporate solvent at 80 °C, and then allow the mixture to react at 300 °C for 10 h. Mix solid, grind and heat at 800 °C for 12 h. | 381 | 45 |
| | Synthesis 3: dissolve sodium carbonate, ammonium dihydrogen phosphate and vanadium acetylacetonate in distilled water. Add this solution to the citric acid solution until a yellow solid is obtained. Stir at 80 °C until a dark green gel is obtained. Drying at 120 °C. Subsequent pre-calcination at 400 °C, 4 h, and final calcination at 850 °C for 12 h. | 381 | 46 |
| | Synthesis 4: disperse vanadium pentoxide and oxalic acid in distilled water and stir at 80 °C to obtain cyanogen solution. Dissolve sodium dihydrogen carbonate and glucose in this solution. Spot dry with injection speed of 300 mL $h^{-1}$ and inlet T 200 °C, outlet T 110 °C. Heat powder at 850 °C in a nitrogen atmosphere. | 381 | 47 |
| | Synthesis 5: dispersion of ammonium metavanadate, sodium carbonate (VWR), and ammonium dihydrogen phosphate in absolute ethanol in a molar ratio of 4 : 3 : 6. Then polyacrylic acid (Sigma-Aldrich) and β-lactose (Sigma-Aldrich) are optionally added. | 381 | 48 |
| $Na_{0.67}[Mn_{0.95}Mg_{0.05}]O_2$ | Solid phase: grind sodium carbonate, manganese trioxide and magnesium oxide, press powder and calcine at 900 °C;15 h in air. | 455 | 49 |
| $Na_{2-\delta}Mn[Fe(CN)_6]$[c] | Dissolve sodium ferrocyanide and sodium chloride in a solution of water and ethanol (solution A). Dissolve manganese(II) nitrate in water (solution B). Add solution B to solution A. Let stand for 2 h, and then filter. Wash precipitate with water and dry at 100 °C for 30 h. | 490 | 50 |
| $Na_{0.61}Fe[Fe(CN)_6]_{0.94}$ [e] | Typical synthesis (not specified), $Na_4Fe(CN)_6$·10$H_2O$ and hydrochloric acid dissolved in deionized water to obtain a homogenous solution. The mixture was maintained at 60 °C for 4 h under vigorous stirring. After filtration the composite was washed with water and ethanol and dried for 100 °C under vacuum for 24 h. | 493 | 51 |
| GO@$Na_{0.81}Fe[Fe(CN)_6]_{0.79}$ [e] | Dissolve sodium ferrocyanide in sulfuric acid and stir for 3 h at 80 °C. Centrifuge and wash the solid with Milli-Q water. Disperse with graphene oxide in water and continue stirring. Treat the slurry with ultrasonic waves, and then perform spray drying. Heat the resulting product at 220 °C for 3 h. | 447 | 52 |
| $Na_{0.9}[Mn_{0.4}Fe_{0.5}Ti_{0.1}]O_2$ | Dissolve sodium acetate, manganese oxide, iron oxide and titanium oxide in a few drops of water and add it to a mixture of NaCl/KCl. Grind and dry at 180 °C for 3 h. Grind again and heat at 800 °C for 10 h in the presence of air. After cooling, wash the solid with water and dry overnight at 60 °C under vacuum. | 308 | 53 |
| $NaFePO_4$ | Sodium carbonate, iron oxalate, and ammonium dihydrogen phosphate are ground and calcined for 5 h under argon. Subsequently, the solid is pelletized and calcined at 600 °C for 10 h under argon. | 410 | 54 |
| $Na_4MnFe_2(PO_4)(P_2O_7)$[d] | Sodium diphosphate, manganese oxalate, iron oxalate and pyromellitic acid are ground. Calcination is carried out at 300 °C for 6 h in air. The product is pelletized and sintered at 600 °C for 6 h. The solid is mixed/milled with pyromellitic acid and heated at 600 °C for 2 h under a controlled atmosphere. | 418 | 55 |
| $Na_2FeSiO_4$[c] | Dissolve iron oxalate, sodium acetate, and citric acid in ethanol and stir at 50 °C. After 3 h, add tetraethyl orthosilicate and continue stirring at the same temperature for 5 h. Then, increase the temperature and continue stirring. Once the gel precursor is obtained, dry it at 60 °C for 12 h. Mix and grind the solid with sucrose. Dry overnight at 100 °C, and then proceed to sintering at 600 °C for 8 h under an argon atmosphere. | 724 | 56 |

Table 2 *(Contd.)*

| Material | Synthesis routes | Reversible specific energy W h $kg^{-1}$ | Source |
|---|---|---|---|
| $Na_2MnSiO_4$[c] | Dissolve tetraethyl orthosilicate in a mixture of ethanol and Milli-Q water (Solution A). Dissolve citric acid in a mixture of Milli-Q water and ethanol (Solution B). Add manganese(II) acetate and stir for 1 h. Combine Solution A and Solution B and stir for 24 h. Remove the solvent, grind the resulting solid, and calcine it at 700 °C for 6 h under an argon atmosphere. Mix and grind the black powder with sodium carbonate. Add citric acid and grind again. Calcine at 750 °C for 8 h under an argon atmosphere. Grind the solid, and then sinter it at 750 °C for 6 h under an argon atmosphere. | 630 | 57 |
| $Na_2MnPO_4F/C$[c] | Synthesis 1: 0.02 moles of $Mn(CH_3COO)_2{\cdot}4H_2O$ and 0.04 moles of citric acid were added to 70 mL of deionized water and stirred for 10 min. Then, 0.04 moles of NaF and 0.02 moles of $NH_4H_2PO_4$ were added to the prepared solution. The resulting mixture was continuously stirred for another 16 h. Subsequently, the homogeneously mixed solution was processed into a solid precursor using a spray dryer. The obtained precursor was compressed into a pellet and sintered in an argon atmosphere at 350 °C for 3 h, followed by heating at 700 °C for 6 h to obtain the product $Na_2MnPO_4F/C$. | 651 | 58 |
| | Synthesis 2: $Na_2MnPO_4F$ was synthesized through a conventional solid-state reaction. Stoichiometric amounts of $Na_2CO_3$ (Aldrich, 99%), NaF (Aldrich, 99%), Mn $(C_2O_4){\cdot}2H_2O$ (Alfa Aesar, Mn 30%), and $NH_4H_2PO_4$ (Aldrich, 98%) were uniformly mixed using a planetary ball mill (Fritsch, Pulverisette7) at 500 RPM for 12 hours. A 10 wt% of pyromellitic acid hydrate (Alfa Aesar, 96%) was added as an organic additive. Then the mixture was heated to 300 °C for 2 h in an ambient argon environment to decompose the precursor. The resulting heated mixture was ground, pelletized, and further heated to 600 °C for 12 h in ambient argon to obtain the $Na_2MnPO_4F/C$ phase. | 651 | 59 |
| $Na_{1.702}Fe_3(PO_4)_3$ | $Na_{1.702}Fe_3(PO_4)_3$ was prepared *via* hydrothermal synthesis. Starting materials were $(NH_4)_2Fe(SO_4)_2{\cdot}6H_2O$ (Aldrich), $H_3PO_4$ (Fisher), and NaOH (Aldrich) and were used as received. Reactants were dissolved in water in a 1 : 1 : 3 molar ratio, and subsequently transferred to a Parr autoclave, which was sealed and heated at 180 °C for 6 h. After cooling to room temperature, the reaction was filtered of the precipitated product. The product was dried to yield a fine powder with a greenish gray color. A SPEX 8000D miller was used to ball-mill the as-synthesized samples of $Na_{1.702}Fe_3(PO_4)_3$. The dried powder of $Na_{1.702}Fe_3(PO_4)_3$ was added to a small amount of ethanol that contained 80 wt% of citric acid (Aldrich). This mixture was sonicated to wet the powder completely with citric acid solution, and subsequently heated at 600 °C under Ar for 5 h to deposit the carbon coating. | 406 | 60 |
| $NaFe_{0.5}Mn_{0.5}O_2$ | $NaFe_{0.5}Mn_{0.5}$ was synthesized by a solid-state reaction from stoichiometric amounts of $Na_2O_2$ (97% Nacalai Tesque), $Fe_2O_3$ (99.7%, Wako Pure Chemical Industries) and $Mn_2O_3$ with the molar ratios of 1 : 1/2 : 1/2, respectively. The mixtures of the samples were thoroughly ground using a mortar and pestle, and then pressed into pellets. The pellets were heated at 700 °C for 36 h in air. Then, they were quenched to room temperature and stored in an Ar filled glove box until use. | 523 | 61 |
| $NaMn_{1/3}Fe_{1/3}Ni_{1/3}O_2$ | A solution of $NiSO_4{\cdot}6H_2O$, $FeSO_4{\cdot}7H_2O$, $MnSO_4{\cdot}H_2O$, and $Na_2C_2O_4$ was added to a stirring solution of sodium oxalate. The co-precipitation solution was continuously stirred for 3 h in ambient air. The solution temperature was kept constant at 70 °C throughout the co-precipitation process. The resultant powder was filtered, washed with Millipore™ water (Barnstead Nanopure), and dried in air at 105 °C. Thereafter, the dried $(Ni_{1/3}Fe_{1/3}Mn_{1/3})C_2O_4$ powder was thoroughly mixed with sodium carbonate respectively in a 2 : 1 mole ratio, and then calcined at 850 °C for 12 h in air. | 481 | 62 |
| $Na_{0.6}Fe_{0.11}Mn_{0.66}Ni_{0.22}O_2$ | The precursor was obtained by co-precipitation method dissolving stoichiometric proportions of $NiSO_4{\cdot}6H_2O$ (Sigma Aldrich, 99%), $FeSO_4{\cdot}7H_2O$ (AnalaR NORMAPUR, analytical reagent) and $MnSO_4{\cdot}5H_2O$ (AnalaR NORMAPUR, analytical reagent) in water and adding an aqueous solution of NaOH drop-wise (50% excess). After extensive rinsing with water, the obtained precursor was dried under vacuum. The powder precursor and NaOH were subsequently mixed in a molar ratio of 1 : 0.685. The mixture was annealed at 500 °C in an air atmosphere, and then as a pellet at 900 °C. Finally, the material was subjected to water treatment. | 324 | 63 |
| $NaMn_{0.5}Ni_{0.5}O_2$ | The $O_3$-$NaNi_{0.5}Mn_{0.5}O_2$ samples were prepared by a sol–gel method based on citric acid. An aqueous solution of a mixture of stoichiometric amounts of sodium nitrate (Alfa Aesar, 99%), manganese(II) nitrate tetrahydrate (Alfa Aesar, 98%), and nickel(II) nitrate hexahydrate (Alfa Aesar, 98%) was added to aqueous critic acid (Alfa Aesar, 99%). The resulting solution was heated on a hot plate at 70 °C and stirred for 6 h to obtain a clear and viscous gel. The resulting gel was dried at 120 °C for 24 h to produce the precursor. Then, the solid precursor was ground and heat-treated at 450 °C in air for 6 h to decompose the nitrate and organics. After cooling to room temperature, the powdered precursor was ground again, pelletized, and then calcined in a muffle furnace at 900 °C for 15 h in an air atmosphere, and then quenched to room temperature. A recalcination process was conducted at 950 °C for another 15 h. | 377 | 64 |

 

**Table 2** *(Contd.)*

| Material | Synthesis routes | Reversible specific energy W h $kg^{-1}$ | Source |
|---|---|---|---|
| $NaMnO_2$ | $NaMnO_2$ was synthesized by solid-state reaction. Stoichiometric amounts of $Na_2CO_3$ (100%, Baker) and $Mn_2O_3$ (98%, Alfa Aesar) were mixed and ball milled in acetone for 6 h at a rate of 300 rpm. The mixture was dried into a powder. About 0.5 g of powder was pressed into a pellet. The pellet was calcined at 700 °C in air for 10 h before it was quenched to room temperature and moved to a glove box filled with argon. | 523 | 65 |
| $NaMn_{0.3}Fe_{0.4}Ni_{0.3}O_2$ | $NaFe_{0.4}Ni_{0.3}Mn_{0.3}O_2$ was prepared *via* the solid-state reaction of $Na_2CO_3$ (3% excess condition; Kanto Chem. Co., Ltd. purity: 99.5%), $Fe_2O_3$ (Wako Pure Chemical Industries Ltd., purity: 99.5%), and coprecipitated $Ni_{1/2}Mn_{1/2}(OH)_2$. The starting materials were mixed using a mortar and pestle, and then pressed into a pellet. The pellet was heated at 800 °C for 24 h in air. | 390 | 66 |
| $Na_{0.6}Fe_{0.20}Mn_{0.65}Ni_{0.15}O_2$ | $Na_{0.67}[Mn_{0.65}Ni_{0.15}Fe_{0.2}]O_2$ was synthesized by a solid-state method. $Na_2CO_3$ (EMD Millipore, Z99.5%), $Mn_2O_3$ (Sigma-Aldrich, 99%), NiO (Sigma-Aldrich,99.8%), and $Fe_2O_3$ (Sigma-Aldrich, Z99%) powders were used as starting materials. A mixture of a stoichiometric number of precursors was pelletized and heated in air at 750 °C for 4 h, followed by a final step at 900 °C for 6 h. Due to the sensitivity of these materials under ambient atmosphere, the sample was subjected to an additional heat treatment under vacuum at 600 °C. | 324 | 67 |
| $Na_{0,6}Ni_{0,22}Al_{0,11}Mn_{0,66}O_2$ | The P2-type layered compound with the nominal composition $Na_{0.6}Ni_{0.22}Al_{0.11}Mn_{0.66}O_2$ (NAM) was prepared by a co-precipitation method dissolving stoichiometric proportions of $Ni(NO_3)_2{\cdot}6H_2O$ (Aldrich, trace metals basis 99 997%), $Al(NO_3)_3{\cdot}9H_2O$ (Aldrich, trace metals basis 99 997%) and Mn $(NO_3)_2{\cdot}4H_2O$ (Sigma Aldrich, Purum p.a., 97.0%) in water and adding an aqueous solution of NaOH dropwise (50% excess). Then, the hydroxide precursor was filtered, washed and dried overnight. Subsequently, a solid-state reaction among the nickel–aluminum–manganese precursor and NaOH in a molar ratio of 1: 0.685 was performed in an air atmosphere at 500 °C for 5 h. A final annealing step at 1000 °C for 6 h was conducted for the pelletized material under an air atmosphere and slowly cooled to room temperature. | 675 | 68 |
| $Na_4MnV(PO4)_3$-rGO | Firstly, $V_2O_5$ and citric acid (2 g) were dissolved in 20 mL of $H_2O$ and stirred at 80 °C to form a clear blue solution (solution A). Then, Na-acetate and GO were also added to solution A. $NH_4H_2PO_4$ and Mn-acetate were dissolved in 10 mL of $H_2O$ (solution B). After stirring at 80 °C for 30 min, solution B was added slowly to solution A and the final solution was continuously stirred at 80 °C for 12 h. Thereafter, the gel was transferred to an oven and heated to 180 °C for 3 h. Then, the dry gel was ground and calcinated under an argon atmosphere at 750 °C for 9 h to obtain a pure $Na_4MnV(PO_4)_3$-rGO composite. | 380[a] | 69 |
| $Na_3MnTi(PO_4)_3$ Synthesis 1[c] | Synthesis 1: NMTP/C@rGO was prepared by a spray-drying approach with post-annealing. 15 mmol $NaH_2PO4{\cdot}2H_2O$, 5 mmol $Mn(CH_3COO)_2{\cdot}4H_2O$, 5 mmol $C_6H_{18}N_2O_8Ti$, and 10 mmol $C_6H_8O_7{\cdot}H_2O$ were dissolved in water. After adding 50 mL of graphene oxide solution (GO, 2 mg $mL^{-1}$) to the above-mentioned solution, the suspension was spray dried. The intermediate collected after spray drying was annealed in Ar for 4 h at 600 °C to obtain NMTP/C@rGO. The control sample, NMTP/C, was synthesized using a similar method without the introduction of GO. NMTP/C@rGO-550 and NMTP/C@rGO-650 were synthesized by varying the annealing temperature to 550 °C and 650 °C, respectively. | 410[a] | 70 |
| Synthesis 2[d] | Synthesis 2: titanium isopropoxide, $TiC_{12}H_{28}O_4$, sodium carbonate, $Na_2CO_3$, ammonium dihydrogen phosphate, $NH_4H_2PO_4$, and manganese(II)acetate tetra hydrate, $(Mn(CH_3OOH)_2)$. | — | Own data |
| $Na_3MnZr(PO_4)_3$ | Carbon-coated $Na_3MnZr(PO_4)_3$ was prepared by the sol–gel method. An aqueous solution of sodium acetate, manganese acetate, ammonium dihydrogen phosphate, zirconium acetylacetonate, and citric acid with a stoichiometric ratio was heated at 80 °C with magnetic stirring to evaporate the water, and then further dried at 100 °C in an oven. The resulting precursor material was ground and sintered at 750 °C for 12 h in a tube furnace under an argon atmosphere. | 402[b] | 71 |

[a] Specific energy is directly from the literature and the average potential is calculated. [b] Specific energy is calculated from the integration of the potential-capacity. [c] 2Na exchange. [d] 3Na exchange. [e] Prussian blue analogues.

word). For example, orthophosphoric acid ($H_3PO_4$) with CAS 7664-38-2 has a hazard classification of Danger H314 for "Skin Corrosion" based on the harmonized classification. Usually, suppliers evaluate their products regarding their potential hazards by reporting them to ECHA *via* a notification. This can lead to a higher number of potential hazards, which are not captured in the harmonized classification of ref. 75. Taking $H_3PO_4$ again as an example, about 200 notifiers also report potential hazards related to H290 (warning, corrosive to metals), H302 (warning, acute toxicity) and H318 (danger, serious eyes damage/eye irritation) besides H314. Additionally, there may be some substances for which only few producers

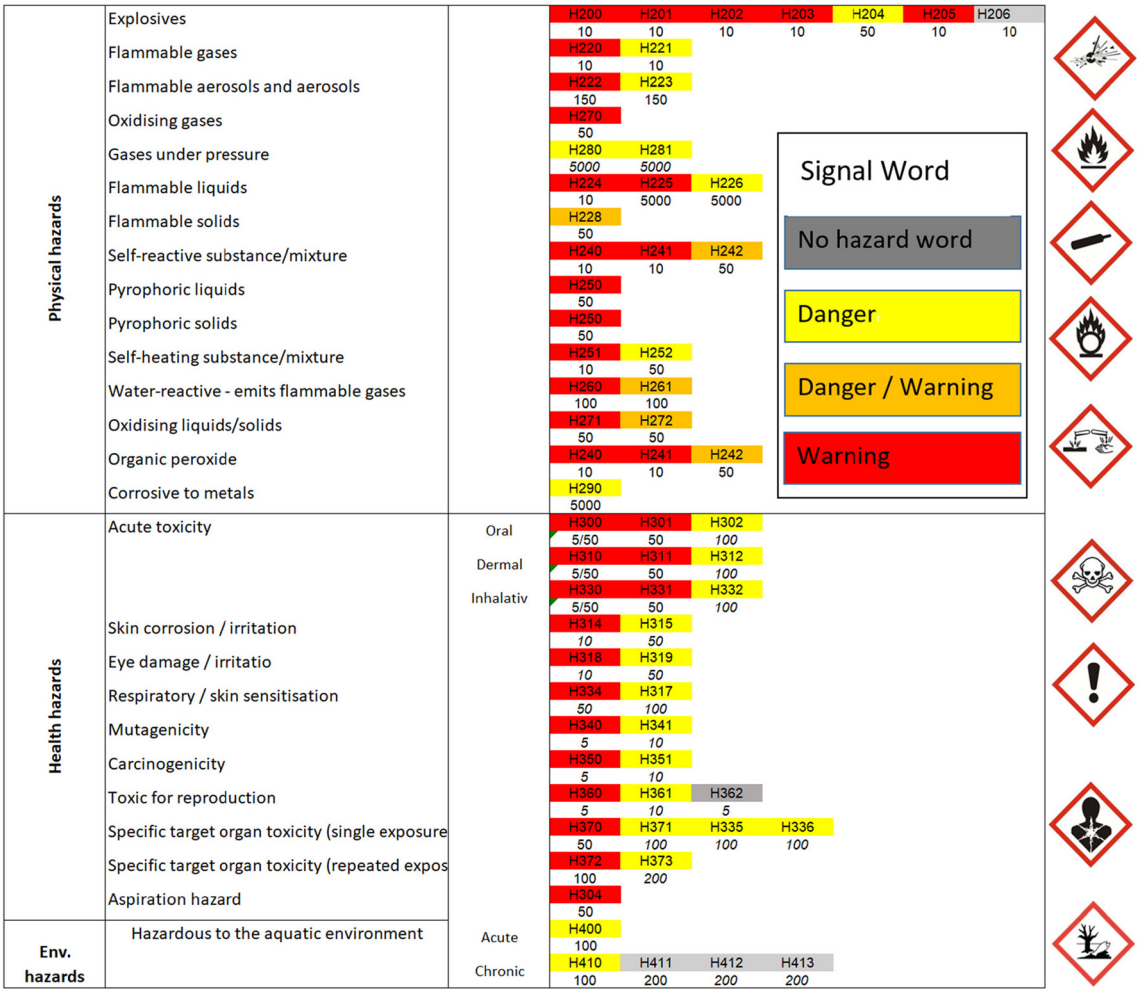


Fig. 2 Hazard traffic light classification with reference quantities (lower tiers, LT, in metric tons) and corresponding GHS pictograms (fitted as best as possible); own draft based on;[17,20] CLP pictograms taken from,[76] orange has been added as a color for yellow/red indications.

have reported hazards given that there is not much experience with them. Thus, potential hazards with over 100 notifications of producers have been included in the HTL assessment to provide a more comprehensive picture of potential hazards and avoid that there is "no hazard" reported. This already represents an extension of the recommendation for hazard substance reporting in the battery passport.[3] It is also important to mention that the identified hazards probably will not directly impact the normal population, rather they can affect workers in corresponding environments (material or battery manufacturing, battery recyclers, *etc.*).[26] Furthermore, the absence of a chemical in the list does not imply that it is non-hazardous.[5]

### Total hazard points

In contrast to HTL, THP is a quantitative method for evaluating the different hazards related to a product,[20] which was first applied for the screening of chloride ion cathode materials.[32] The THP are based on the classification according to the HTL but go a step further by creating a dimensionless sum-indicator for all hazards. Originally, the core of this method was developed for the German Environmental Agency (UBA).[19,20] Here, for each material, their hazard score was calculated starting from the HTL analyses. The THP are based on quantity thresholds that apply to hazardous substances (in tons), which vary among the different categories of dangerous substances,[20] and require special safety conditions if exceeded (Seveso III Directive[23] for lower tier (LT), as depicted in Fig. 2). If the mass surpasses the LT, a major accident prevention policy (MAPP) is required. The lower the value for an LT, the higher the hazard. The LT values in tons for different H-phrases according to[17] were used for the evaluation of the cathodes (see ESI†). In some cases, two values were named, and given that different categories exist here (*e.g.*, H300), the lower value was used (*e.g.* for H330 the lower value of 5 was used). This may lead to some uncertainty in the assessment, given that some materials may be overestimated regarding their hazard statements.

Here, the mass shares of each CAM were calculated, each with a certain hazard and a corresponding lower tier of $LT_1$,

 

$LT_2$, and $LT_3$. The results are depicted in hazard points HP per kg and kW h of CAM. For more details on the methods, see ref. 20. Subsequently, the hazard points are calculated based on LTs, where the total hazard point is the sum of the hazard points of each hazard statement. Again, the LTs are based on the hazard statements reported by more than 100 notifications from companies *via* the summary of classification and labelling sheets from ECHA, and thus may change over time.[73]

### Life cycle assessment

The life cycle assessment (LCA) approach takes a different viewpoint and looks at the potential toxic impacts of the materials along the whole production chain up to the precursor material, *i.e.*, considering all upstream impacts. The screening of the CAM is based on the impact assessment method recommended by the European Commission for the Environmental Footprint method.[22] In turn, it relies on the Use-Tox® approach developed under the support of the United Nation Environmental Program and SETAC Life Cycle Initiative for calculating the potential impact of chemicals on the ecosystem and human health.[77] Also, the Use-Tox® model relies on data on substance properties from the implementation of the REACH database, plus information from the OpenFoodTox Database (OFT-DB) and the Pesticide Property Database (PPDB) by.[78] For the present screening, the two categories "human toxicity, cancer" and "human toxicity, non-cancer" are aggregated into a single score and quantified in CTU (comparative toxic units).

For the inventory data, the ecoinvent database was used (v3.9) in combination with the LCA software OpenLCA.[79] The CAM not directly contained in the ecoinvent database were modelled based on their corresponding precursors following the most common synthesis route derived from the literature. In this case, the amount of precursor was obtained *via* stoichiometric calculation based on the specific synthesis reactions. Single precursors that are not contained in the ecoinvent database, such as vanadium pentoxide, are taken from publications who develop specific datasets for substances.[80] This may introduce some bias given that the modelling assumptions were not necessarily identical. For the modelling of the CAM synthesis routes, only the principal educts were considered, disregarding auxiliaries and other inputs such as energy. This constitutes a certain mismatch with the modelling approach used in the ecoinvent database (which follows a life-cycle approach considering all inputs until the final product), but is deemed sufficient for the present screening approach given that the contribution of auxiliary inputs to the total CAM impacts are typically low, while the energy demand for calcination is similar across different CAM.[7] This approach was consistently applied to all assessed CAM. A detailed list of all considered precursors and their potential impacts is provided in the SI.

## Results

As explained before, this assessment is not aimed at the precise determination of the impacts of a final battery or CAM. Alternatively, it is intended as a guide for supporting an early-stage comparison and hotspot analyses of materials that are under development, where a high uncertainty is given both for the other components of the battery cell (final composition, used materials...) and for most of its electrochemical properties (specific energy, efficiency...). Therefore, the results should be seen as explorative with the aim of providing a first and rapid orientation toward promising material candidates, unveil hotspots and identify the corresponding need for more detailed assessments. Moreover, this work can serve as a contribution to the ongoing discussion on a safe and sustainable-by-design approach to chemicals.[4] A requirement of the EU Battery Regulation introduces mandatory testing of hazardous substances, and thus the results provided herein can help to identify the corresponding substances.[3] In the following, all impacts are displayed per mass unit of material. However, to reflect the properties of different CAM, these are related to their theoretical specific energy, resulting in a functional unit of HTP (g) per kW h as in Rodriguez *et al.*, 2016,[20] which allows a direct comparison of the different CAMs.

### Hazard traffic lights

The HTL provide a first overview of the potential hazards of the CAM precursors and the selected solvents. They represent a qualitative approach that allows a first impression of the used precursors, as indicated in Fig. 3. Here, a selection of 28 SIB and three reference LiB is provided to demonstrate the HTP. On the left side of the figure, all hazard statements with their corresponding classification are provided. The HTL for all analyzed CAM, including the list of all substances, related identifiers and hazard classes, are provided in the SI, as recommended by.[3]

The harmonized statements are also marked with a checkmark based on the latest downloadable version with harmonized classification and labelling up until the "17$^{th}$ Adaptation to Technical Progress", which contains around 4330 substances.[75] Here, all hazards are harmonized throughout the EU, which includes several steps until the inclusion into Annex IV.[81] It can be clearly seen that the use of an extended classification *via* notifications leads to a significantly higher number of hazard statements within HTL. The threshold for the number of declarations was set to >100, but the figure would look significantly different with a lower threshold of, *e.g.*, 50 notifications. This significantly depends on the preference of the analyst, where it is reasonable to set a lower threshold for very early TRL technologies. For example, for specific SIB precursors that are not (yet) produced on a large scale, only a few statements has been reported. However, this does not mean that the corresponding substances do not inhibit hazards, rather there are only very few notifications. This means that lower TRL technologies may have a lower score than established technologies. However, this is not an issue in this approach, rather it constitutes a general data problem for screening activities. All the selected CAM show potential hazards, in particular in the field of health hazards, where all have impacts on acute toxicity (H302), eye damage

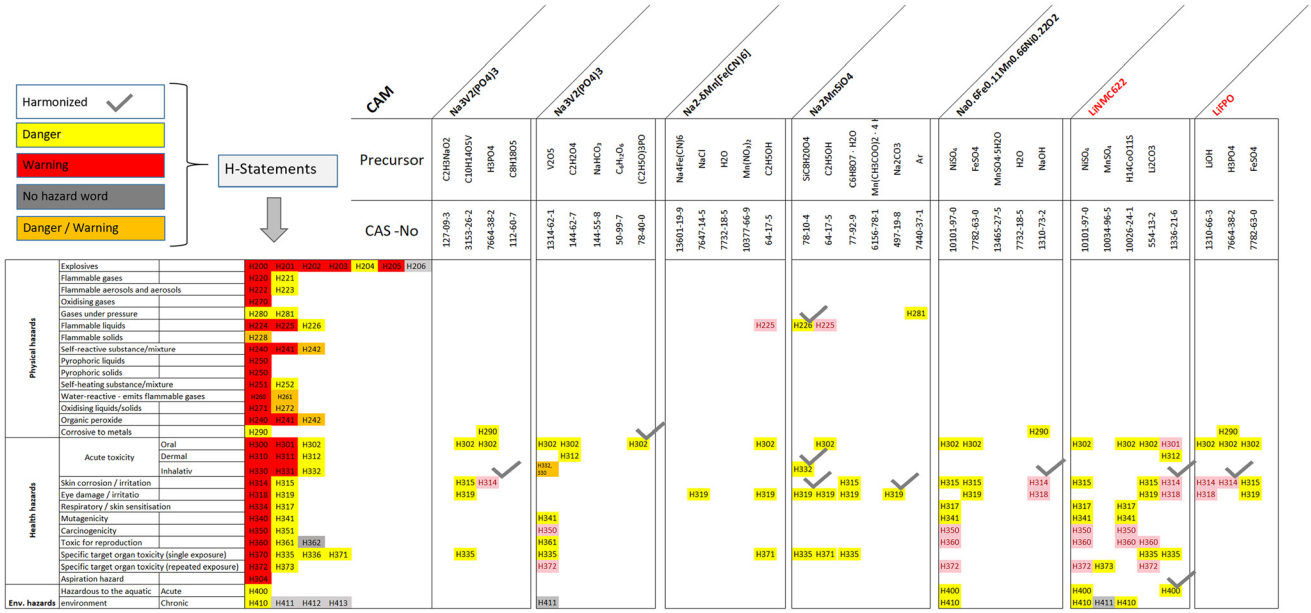


**Fig. 3** Example of HTL for five selected SIB and two state of the art LiB for comparison (labeled in red). The orange category has been changed due to operationalization, as it was originally a yellow/red field. Harmonized statements are marked with a checkmark.

(H319) and specific target organic toxicity (H335). A few SIB alternatives also pose physical hazards such as $NaFePO_4$, $NaMnO_2$ and $Na_2FeSiO_4$.

Finally, it does not matter that there are more "danger" notifications for NMC and LFP given that the purpose of the HTL is not to compare LIB or SIB; they serve as a base to identify potential hotspots and ideally find alternative precursors that are easier to handle. Furthermore, the provided tables show that each SIB precursor has specific impacts and that SIB share some of the same precursors with LIB, *e.g.*, nickel sulfate in the case of NMC622 and $Na_{0.6}Fe_{0.66}Ni_{0.22}O_2$, which has multiple hazard warnings from danger to warning.

$Na_3V_2(PO_4)_3$ represents an interesting case where five specific synthesis routes with three different precursors are used. One variant is based on $V_2O_5$, which is linked to potential hazards, *e.g.*, warning with a red indication for specific target organ toxicity (H372). The other identical alternative is based on oxobis(pentane-2,4-dionato-*O*,*O*)vanadium, which is among other things labeled as "danger" corrosive to metals (H290) in yellow. Both precursors share the danger label for acute oral toxicity (H302). These comparisons can be applied to support the process of material selection for further development.

## Total hazard points (THP)

The results for the THP calculus are provided in Fig. 4, with Fig. 4A showing the results per kg of CAM and Fig. 4B per kW h of specific capacity, thus accounting for the different amounts of CAM required for providing the same cathodic energy capacity. The chemistries are classified into oxidic and polyanionic CAM. Additionally, state-of-the-art LIB are included for exemplary comparison with NMC111 and NMC622 for the oxidic and LFP for the polyanionic type CAMs. In Fig. 4B, some bars are cut off, and in this case, the value is indicated in a white textbox. Fig. 4C provides the relative contributions of the precursors to the total impact, which are independent of the functional unit (*i.e.*, per kg or kW h).

In the case of both LIB and SIB, the results can vary strongly depending on their chemistry, selected synthesis routes, and precursors. A second important component is the specific energy, with a lower energy density resulting in a higher demand for the corresponding precursors. In general, CAM that include precursors containing Ni, Co and V lead to very high THP. Here, for LIB, in particular NMC111, Co is one of the biggest contributors due to the high score obtained by cobalt sulphate. In the case of the polyanionic CAM, vanadium is the most important driver for THP, although it varies significantly depending on the used precursors. The results for the different $NaV_2(PO_4)_3$ cells lead to comparable results when vanadium-acetylacetonate and vanadium pentoxide are used, but higher THPs when using ammonium metavanadate and vanadium pentoxide due to their dangers related to acute toxicity (oral and inhalation) with very low LTs of 5. For some CAM such as the Prussian blue analogue group, they have no impacts. This is due to the fact that either no further precursor has been named or no notification or registered hazard is available for the analyzed precursor, which can change with future updates and will be addressed in the sensitivity analyses. Finally, it has to be considered that the results provided in Fig. 4 are based on the precursors identified in Table 2 and only valid for these specific synthesis routes. Thus, with other routes using different precursors with different CAS numbers, the results may change significantly.

As explained before, it is important not to compare the SIB CAM with LIB state-of-the-art technology. The THP can depend

 

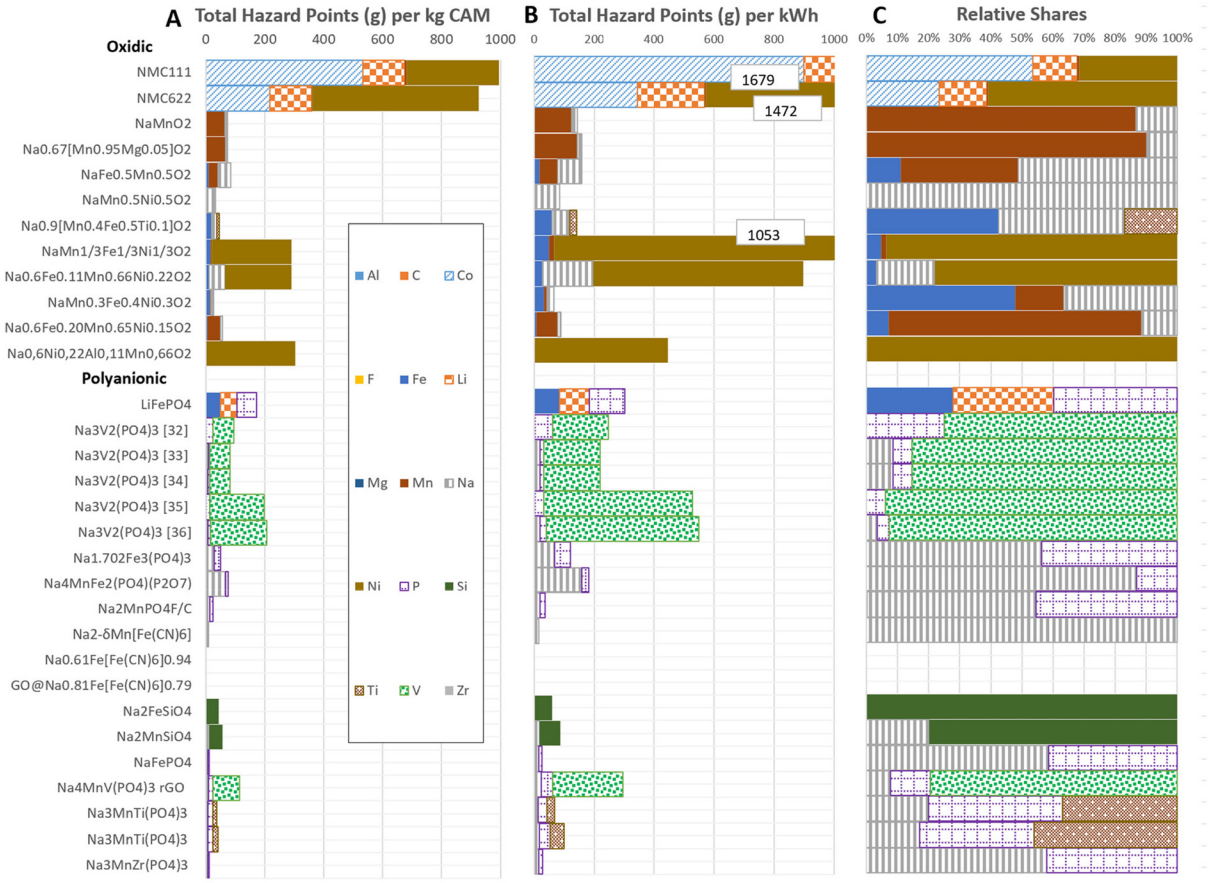


**Fig. 4** THP per kg (A) and kW h (B) of CAM. Corresponding shares of THP (C), where absolute numbers are provided in boxes for the chemistries which are cut in Figure A and B.

to a certain degree on the TRL of technology, as explained before. A low THP may just result from a low number of notifications due to the limited use of a rather new precursor. Nevertheless, the THP are expected to provide initial insights into potential hazards.

### Life cycle assessment

The results for the LCA-based toxicity screening are displayed in Fig. 5 and are structured in the same way as the result for the THP in Fig. 4. Consistent with the latter, the specific energy strongly influences the overall impact when the results are compared to the mass-based assessment. The high potential impact obtained for the NMC cathodes and all the vanadium-containing CAM is notable. In the case of the former, this is mainly caused by the direct emissions from cobalt mining and its processing into cobalt hydroxide, with heavy metal emissions in the air, particularly mercury and arsenic being the main contributors. For the same reason, although to a lower extent, nickel is also an important contributor to the toxic impacts, situating all the nickel-containing CAM in the middle field.

Similarly, around half of the very high potential toxicity impacts of the vanadium-containing CAM is caused by direct emissions along the process chain, and in this case mainly from the processing of the vanadium-bearing cast iron and vanadium slag, with significant emissions of lead and mercury. The other half is driven by the electricity to power the electric arc furnaces, with the vanadium production process situated in South Africa, where a high share of coal power is used with the corresponding emissions of arsenic, lead, and mercury from coal combustion. In this case, it should be noted that the corresponding inventory is specific and developed for a hypothetical site and production pathway situated in South Africa, and not necessarily representative of the global average.[80] Also, it does not necessarily rely on the same modelling framework as the datasets taken from the ecoinvent database. However, even if zero impacts were assumed for the energy input, vanadium would still be situated among the highest impact precursors.

Unlike global warming impacts, where sodium precursors were found to have negligible impacts in a previous work, this is not the case for toxicity. Here, depending on the specific sodium-providing precursor used, the toxicity impacts from the precursors are relevant and can even be higher than that of the corresponding lithium precursors. However, this is not caused by sodium itself but its corresponding carrier component, such as in the case of sodium oxalate, where oxalate causes the high impacts. In most cases, the impacts are, as in

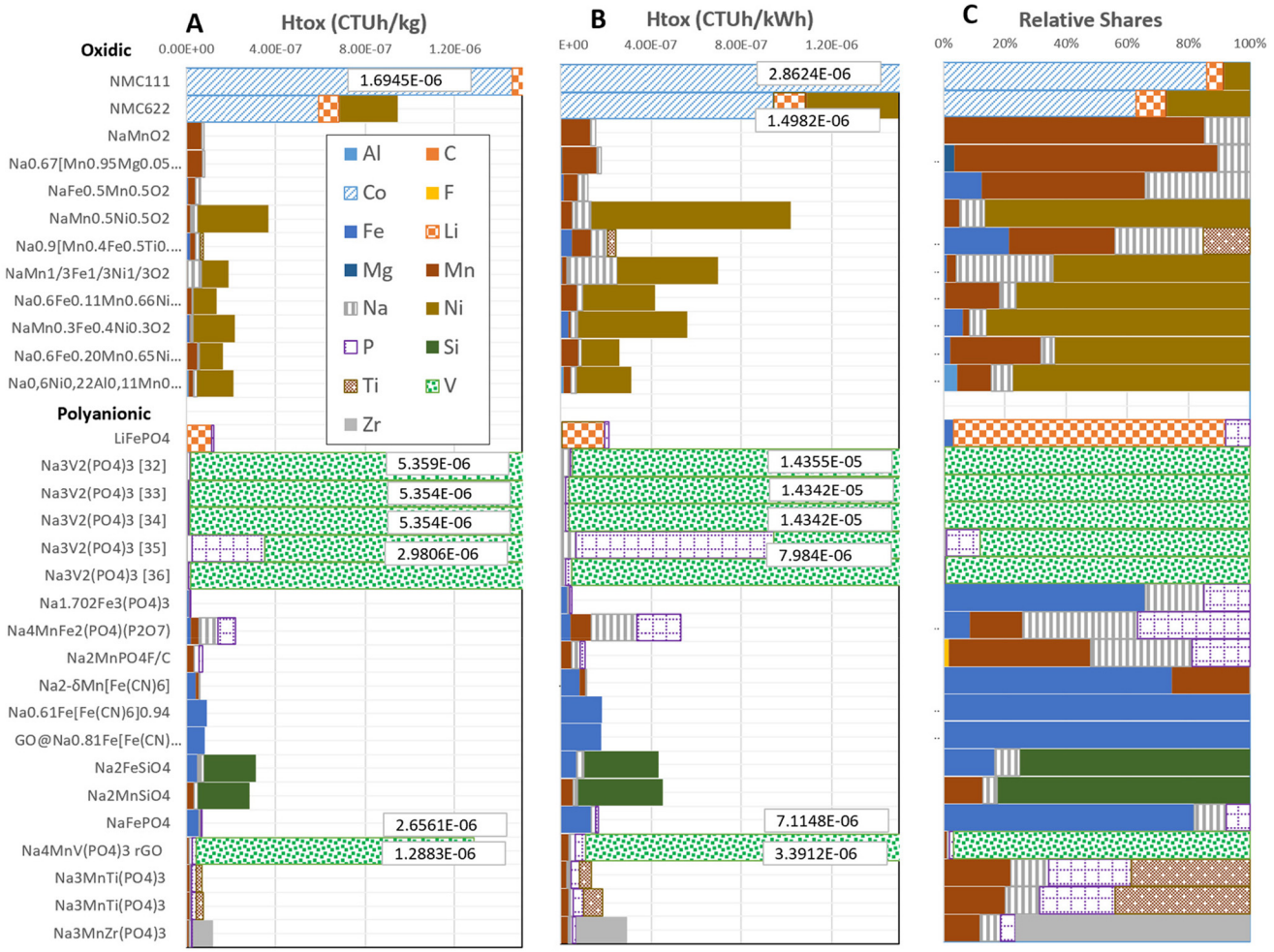


**Fig. 5** HTox per kg (A) and kW h (B) of CAM. Corresponding shares of HTox (C), where the absolute numbers are provided in boxes for the chemistries, which are cut in Figure A and B.

the case of the THP, mainly driven by V-, Ni- and Co-based precursors. The comparison of LIB with the SIB alternatives showed that the Na-based precursors tend to have lower impacts than Li-based precursors, which has to be analyzed in detail *via* a full LCA.

### Qualitative comparison

Both quantitative approaches, THP and LCA (HTox), are compared in Fig. 6. It is difficult to compare both methods due to their different scales, system boundaries and calculation procedures. However, Fig. 6 still provides some interesting insights and can help to identify potentials hazard hotspots considering potentially missing data for LCA or THP. In the case of the CAMs from the group of manganese-based layered oxides and polyanionic Prussian blue analogues, lower hazards and impacts can generally be observed. In contrast, for the vanadium-containing CAM, the correlation between HTox and HTP is low. Here, all the V-containing CAM show a comparably high HTox impact, while only for two cases this is correlated with THP. This is the case for the $NaV_2(POV_4)_3$ and $Na_4MnV(PO_4)_3$ variants due to the use of the same precursor, ammonium metavanadate, which can also be used to produce $V_2O_5$. A low correlation between THP and HTox is also obtained for NMC111 and NMC622, where the results provide a very different picture, whilst in the case of $LiFePO_4$, a comparable tendency for THP and HTox can be observed. However, it also has to be considered that the HTox impacts for the vanadium components are based on an inventory for $V_2O_5$ taken from a scientific publication, and not from the ecoinvent database as for most of the remaining materials.

A detailed assessment of the V-containing precursors was carried out to understand the reason for this very different picture of HTox and THP. The results are displayed in Fig. 7 for the HTL, THP and HTox as the life cycle impact assessment (LCIA) method. Firstly, the HTL show that all three CAM pose several health hazards, as shown before. All three precursors are hazardous, with effects on specific target organ toxicity (H335). $V_2O_5$ and $NH_4VO_3$ pose hazards of acute toxicity and H341, mutagenicity. Both inhibit hazards for H330, acute inhalative toxicity, with a very low LT. Therefore, the THP

 

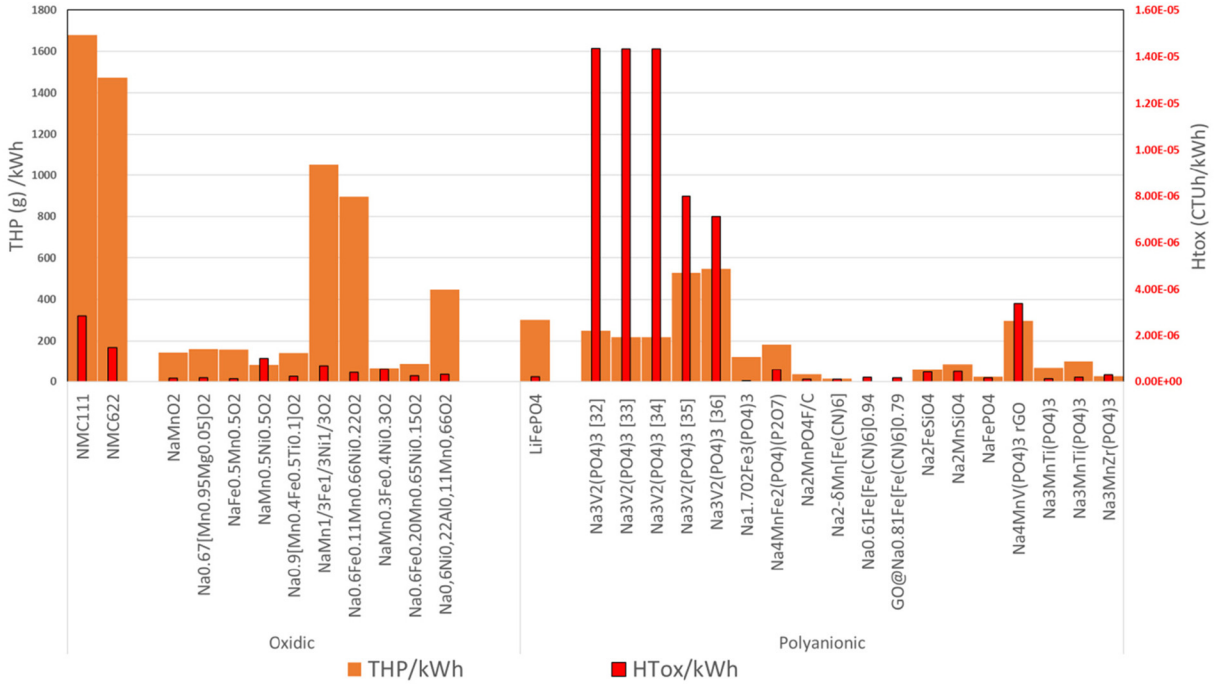


**Fig. 6** Comparison of THP (left *y*-axis) and HTox (right red *y*-axis) results.

impact of these precursors is high, in particular for $V_2O_5$, whilst for the other V-containing precursor $C_{10}H_{14}O_5V$, only a lower hazard score was achieved. The other impacts of $C_{10}H_{14}O_5V$ are 'corrosive to metals' (H290), and $V_2O_5$ is hazardous to the aquatic environment (H411). As explained before, for the LCA, some precursors are not available in the ecoinvent database, and thus were modelled based on the assumed synthesis of further precursors. This was also the case for $C_{10}H_{14}O_5V$ and $NH_4VO_3$, which are both based on $V_2O_5$. As explained before, the impact of $V_2O_5$ has the highest share and poses the reason for the high impact. This may be due to the assumption that vanadium is obtained from titanomagnetite ores.[80] A detailed assessment of other vanadium precursors and synthesis routes can be found in.[29]

Finally, although benchmarking was not the ultimate goal of this assessment, all CAM-variations were compared qualitatively using the THP and HTox results, as shown in Table 3. A simple rescaling of THP and HTox was carried for this purpose, normalizing both to the same value range (a 1–3 scale), where 1 indicates medium risk, 2 high risk and 3 very high risk.[34] Then, the rescaled results were combined using the weighted sum method (WSM) using equal weights for both indicators. Although this is a comparably simple approach, this is considered appropriate based on the very mixed TRLs and data availabilities and the strong qualitative character of the comparison. The weighted sum was the basis for the final ranking of the different CAM. In addition, a composite score was built from the average of the THP and HTox, providing a better understanding of the overall performance of each CAM. As before, NMC for LiB and V-containing precursors for SiB are ranked last, with the corresponding high final qualitative hazard and toxicity risks. There are no results available (NA) for Prussian blue analogues, given that there are no hazards indicated based on the selected thresholds. It should be noted that no green or low risk indication is provided, given that it is hardly possible to do so based on the very different data quality and the different development stages of the considered CAM.

# Discussion

### Sensitivity analyses for selected CAM

For some CAM, no THP score was determined using the presented approach (based on the harmonized hazards and the extended assessment with a threshold of >100 notifications). This is particularly apparent for the Prussian blue analogues, where only a few notifications are available for sodium ferrocyanide ($Na_4Fe(CN)_6$), with the consequence that there is no THP for this CAM with the used threshold (TH), suggesting that there is no hazard related to this precursor. However, if the threshold for the number of notifications was set differently, the results would change. This effect is shown in Fig. 8 for sodium ferrocyanide ($Na_4Fe(CN)_6$), where alternative thresholds are used instead of the default >100. A low number of notifications may occur when a certain material is not used widely, and consequently not registered in SCIP to date. Thus, the differences in HTL when using the default threshold of 100 with one of >30, >20 and >1 (minimum) are compared in Fig. 8A. Fig. 8B shows the different THP scores for this

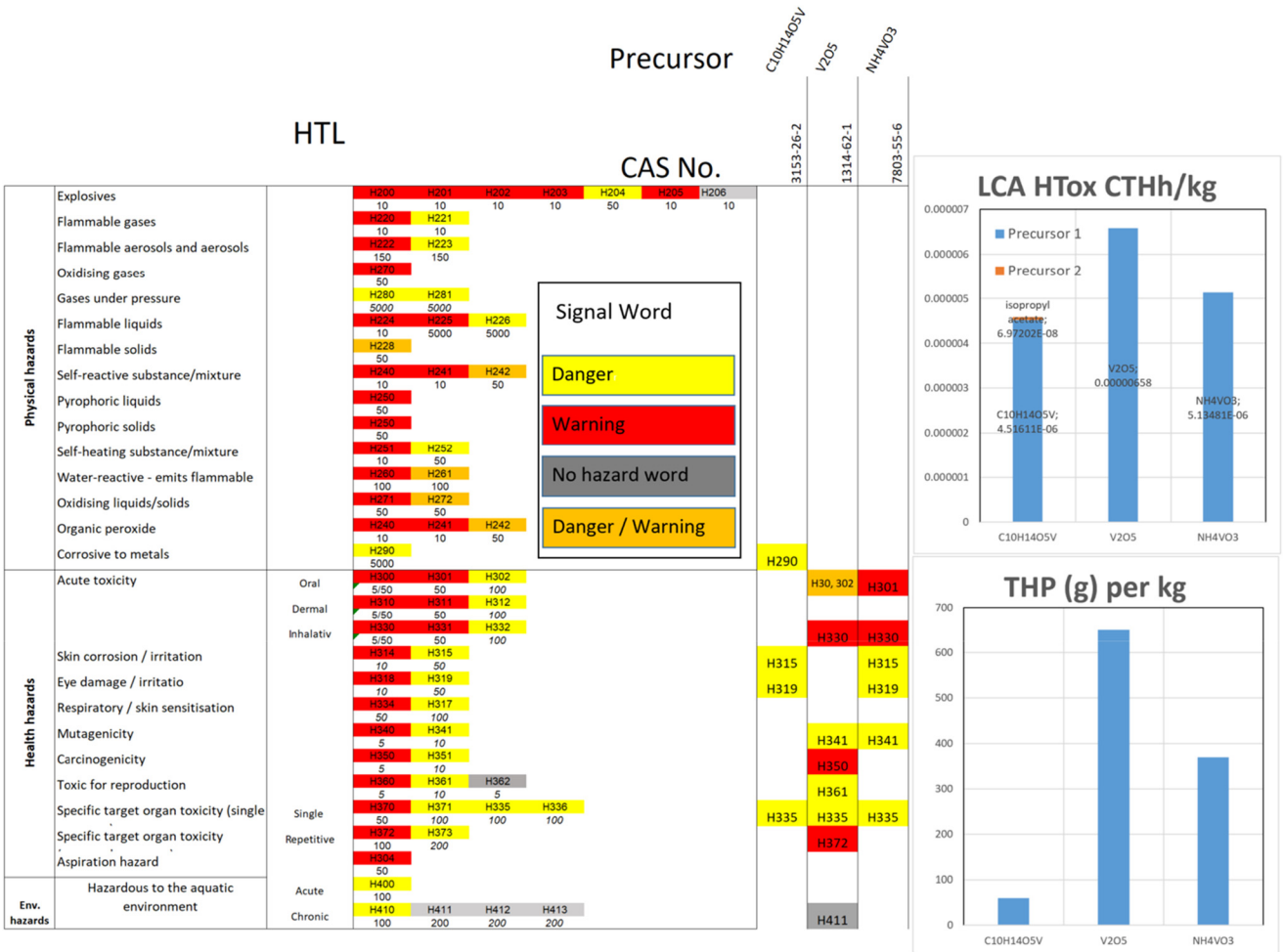


Fig. 7 Comparison of HTL, LCA HTox and THP of different vanadium-providing precursors for the synthesis of $Na_3V_2(PO_4)_3$.

material, with the THP increasing strongly for a lower threshold. This change in TH may lead to high values for Prussian blue analogue precursors on a CAM level, leading to higher impacts per kW h (over a THP of 2770, not displayed here). This is mainly due to the hazards in the entire group of acute toxicity, showing that the selection of the corresponding thresholds is critical and has to be checked accordingly in each assessment. Interestingly, there are over 200 notifiers without classification for this substance. In addition, other sources should be cross checked if there is no hazard for a certain material, for example in,[82] where further hazards are indicated (irritant). As mentioned before, in the case that a substance is not classified anywhere, its self-classification has to be carried out in frame of the Battery Passport.[3]

### Methodological challenges and limitations

As stated before, there is no standard available for hazard and toxicity assessments for early stage screening to support sustainable by design approaches considering the requirements formulated in the EU Battery Regulation. As shown in the literature review, a set of different methods has been applied directly or indirectly for materials screening towards hazards. However, the methods used herein aim to provide first feedback *via* the identification of hazard hotspots to material developers within a very short time frame and aid decision-making toward the selection of different materials, in particular CAM for SIB. These assessments only represent a first step for further assessments[34] and should be combined with further indicators such as global warming potential or even social aspects such as local employment or forced labour. In addition, the presented approach should also consider different life cycle stages. Therefore, there are some limitations that must be addressed, which sometimes are not directly related to the methods and are relevant in this field in general and remain unsolved in named regulations. Specifically, the assessment carried out herein is based on theoretical values for the specific energy on the CAM level and only considers a part of the entire cell, disregarding the interplay among the cathode, electrolyte, separator, and anode (components that all have to be included in the Battery Passport). Also, as mentioned before, the provided list of SIB cathodes is not necessarily comprehensive, given that there are other materials that can be considered promising for future assessments.[36,39]

 

**Table 3** Qualitative comparison of selected CAM with rescaled values (1–3), weighted sum using equal weights, corresponding rankings and an average composite hazard toxicity risk score

| SIB CAM Oxidic | THP/kW h values | Htox/kW h values | THP/kW h rescaled | Htox/kW h rescaled | Weighted sum score (equal weights) | Ranking | Composite hazard – toxicity risk |
|---|---|---|---|---|---|---|---|
| $NaMnO_2$ | 143 | $1.6 \times 10^{-7}$ | 1.1 | 1.0 | 0.1 | 12 | 1.1 |
| $Na_{0.67}[Mn_{0.8}Mg_{0.2}]O_2$ | 128 | $1.6 \times 10^{-7}$ | 1.1 | 1.0 | 0.1 | 11 | 1.1 |
| $NaFe_{0.5}Mn_{0.5}O_2$ | 159 | $1.2 \times 10^{-7}$ | 1.2 | 1.0 | 0.1 | 13 | 1.1 |
| $NaMn_{0.5}Ni_{0.5}O_2$ | 85 | $1.0 \times 10^{-6}$ | 1.1 | 1.1 | 0.1 | 15 | 1.1 |
| $Na[Mn_{0.4}Fe_{0.5}Ti_{0.1}]O_2$ | 145 | $2.5 \times 10^{-7}$ | 1.1 | 1.0 | 0.1 | 14 | 1.1 |
| $NaMn_{1/3}Fe_{1/3}Ni_{1/3}O_2$ | 1053 | $7.0 \times 10^{-7}$ | 2.2 | 1.1 | 0.2 | 22 | 1.7 |
| $Na_{0.6}Fe_{0.11}Mn_{0.66}Ni_{0.22}O_2$ | 896 | $4.2 \times 10^{-7}$ | 2.1 | 1.1 | 0.2 | 21 | 1.6 |
| $NaMn_{0.3}Fe_{0.4}Ni_{0.3}O_2$ | 67 | $5.6 \times 10^{-7}$ | 1.1 | 1.1 | 0.1 | 9 | 1.1 |
| $Na_{0.6}Fe_{0.20}Mn_{0.65}Ni_{0.15}O_2$ | 88 | $2.6 \times 10^{-7}$ | 1.1 | 1.0 | 0.1 | 6 | 1.1 |
| $Na_{0.6}Ni_{0.22}Al_{0.11}Mn_{0.66}O_2$ | 447 | $3.1 \times 10^{-7}$ | 1.5 | 1.0 | 0.1 | 19 | 1.3 |
| **Polyanionic** | | | | | | | |
| $LiFePO_4$ | 303 | $2.1 \times 10^{-7}$ | 1.3 | 1.0 | 0.1 | 17 | 1.2 |
| $Na_3V_2(PO_4)_3$ | 249 | $1.4 \times 10^{-5}$ | 1.3 | 3.0 | 0.2 | 28 | 2.1 |
| $Na_3V_2(PO_4)_3$ | 219 | $1.4 \times 10^{-5}$ | 1.2 | 3.0 | 0.2 | 27 | 2.1 |
| $Na_3V_2(PO_4)_3$ | 219 | $1.4 \times 10^{-5}$ | 1.2 | 3.0 | 0.2 | 26 | 2.1 |
| $Na_3V_2(PO_4)_3$ | 529 | $8.0 \times 10^{-6}$ | 1.6 | 2.1 | 0.2 | 24 | 1.9 |
| $NaFePO_4$ | 25 | $1.7 \times 10^{-7}$ | 1.0 | 1.0 | 0.1 | 1 | 1.0 |
| $Na_{1.702}Fe_3(PO_4)_3$ | 121 | $5.0 \times 10^{-8}$ | 1.1 | 1.0 | 0.1 | 8 | 1.1 |
| $Na_4Mn_3(PO_4)(P_2O_7)$ | 170 | $4.9 \times 10^{-7}$ | 1.2 | 1.1 | 0.1 | 16 | 1.1 |
| $Na_2MnPO_4F$ | 36 | $1.1 \times 10^{-7}$ | 1.0 | 1.0 | 0.1 | 2 | 1.0 |
| $Na_{2-\delta}Mn[Fe(CN)_6]$ | 352 | $5.1 \times 10^{-8}$ | 1.4 | 1.0 | 0.1 | 18 | 1.2 |
| $Na_{0.61}Fe[Fe(CN)_6]_{0.94}$ | NA | $1.8 \times 10^{-7}$ | NA | 1.0 | NA | NA | NA |
| $Na_{0.81}Fe[Fe(CN)_6]_{0.79}$ | NA | $1.8 \times 10^{-7}$ | NA | 1.0 | NA | NA | NA |
| $Na_2FeSiO_4$ | 60 | $4.3 \times 10^{-7}$ | 1.0 | 1.1 | 0.1 | 5 | 1.0 |
| $Na_2MnSiO_4$ | 86 | $4.5 \times 10^{-7}$ | 1.1 | 1.1 | 0.1 | 10 | 1.1 |
| $Na_3V_2(PO_4)_3$ KIT | 549 | $7.1 \times 10^{-6}$ | 1.6 | 2.0 | 0.2 | 23 | 1.8 |
| $Na_4MnV(PO_4)_3$ | 297 | $3.4 \times 10^{-6}$ | 1.3 | 1.5 | 0.1 | 20 | 1.4 |
| $Na_3MnTi(PO_4)_3$ | 69 | $1.4 \times 10^{-7}$ | 1.1 | 1.0 | 0.1 | 4 | 1.0 |
| $Na_3MnTi(PO_4)_3$ | 100 | $1.9 \times 10^{-7}$ | 1.1 | 1.0 | 0.1 | 7 | 1.1 |
| $Na_3MnZr(PO_4)_3$ | 27 | $2.9 \times 10^{-7}$ | 1.0 | 1.0 | 0.1 | 3 | 1.0 |

Qualitative risks – color indication: Medium, High, Very high

Typically, the specific energy on a cell level is significantly lower than on the CAM level.[8] In addition, the results do not reflect in any way the use or end of life phase. For example, a high cycle lifetime and high recyclability of a cell can counterbalance potential burdens on a production level.[7,83] Thus, this screening should not be used to identify the best option, but rather to identify the group of good options for further investigations and identification of hazard hotspots. Also, synthesis routes can vary strongly in terms of process and used precursors, and thus should always be analyzed for each particular case. The synthesis routes presented herein are mostly based on individual lab-scale processes, and thus not representative, for example, the large-scale production of SIB. Another challenge shared by all applied methods here relates to the correct precursor selection with the corresponding CAS number, which is often only partially possible due to the limited information provided in some related publications on the exact synthesis routes and precursors used for the CAM synthesis. This can lead to a skewed picture, where some authors provide a high degree of information with all used precursors, potentially leading to a higher hazard or HTox impact. Also, as stated before, the picture for low TRL technologies as SIB can change very fast when a certain precursor is used more frequently, resulting in a higher number of notifications regarding potential hazards. Here, an extended consideration of hazards beyond the harmonized ones was used (over 100 notifications) to gather a more conservative picture. This value was used after internal discussion with experts, but there is no guideline where to set this value. Setting a lower value, *e.g.*, 30 will potentially result in a higher impact for HTL and THP for some materials but is rather steady for most alternatives. This is especially true for emerging materials, with rather lower production quantities shown for sodium ferrocyanide ($Na_4Fe(CN)_6$)-containing materials. In any case, there is no blueprint for this threshold, and alternative ways of classification must be carried out in case of no substance notification. In addition, despite all the challenges, there is simply no alternative set of methods available for hazard screening of low TRL and actually market ready battery cells.

Finally, only precursors but no intermediate and final products (here CAM) were evaluated regarding their hazards. This can lead to different results depending on whether a precursor is directly purchased or synthesized from other different precursors. One of these substances that requires more investi-

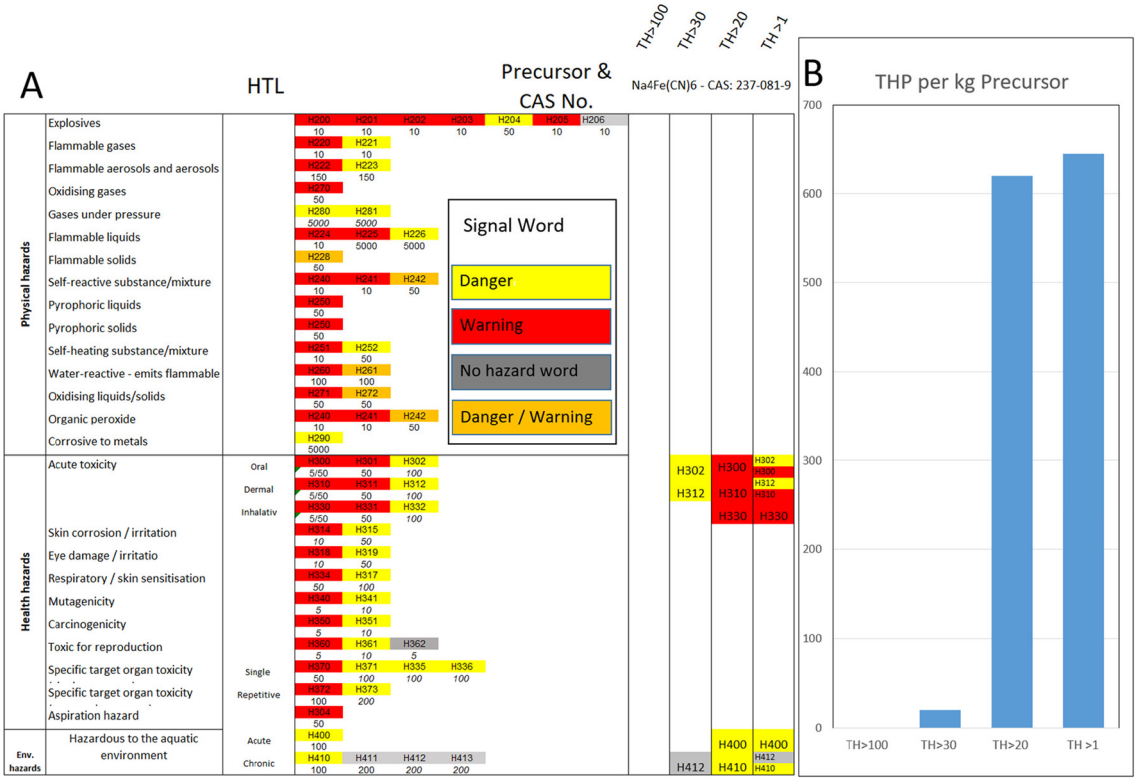


**Fig. 8** Comparison of HTL (A) with different thresholds for sodium ferrocyanide ($Na_4Fe(CN)_6$), (B) resulting THP and their combination for thresholds TH > 30, > 20, > 1 and impacts on a kg base.

gation, but that has not been included here, is fluorinated substances (per- and polyfluoroalkyl substances (PFAS)). These are part of LiB and SiB components (binder, electrolyte, additives and separator), and thus have to be evaluated cautiously.[84] It is expected that PFAS will be considered more in an updated version of the ECHA database in 2024. Also, hazards related with other life-cycle stages are out of scope of the present approach. For instance, toxic substances different than the CAM educts might be released as a result of thermal treatment in the recycling stage or of accidental thermal runaway or fire, such as cynaides from the mentioned Prussian blue analogues.

## Conclusion

The aim of our assessment was to provide an approach for the prospective screening of potential hazards of substances used as SIB and LIB cathode active materials (CAM). Specifically, it aimed to contribute to the development of still widely missing indicators and innovative risk assessment tools considering current requirements regarding hazardous substances, *e.g.* within the EU-Battery Regulation and the corresponding product labeling requirements. In addition, monitoring hazards in the early development phase of new CAM materials can help realize a sustainable-by-design approach to battery cells. For this purpose, three different sets of methods were applied, as follows: (i) the hazard traffic lights (HTL), which provide a qualitative quick picture of potentially problematic substances used for CAM production, (ii) the total hazard points (THP method), which builds on HTL but incorporates a quantitative, and thus comparable component, and (iii) a life cycle assessment-based impact category that quantifies potential human toxicity impacts of materials (HTox) caused along their production chains. Finally, a qualitative comparison and final hazard risk are present for the different SIB and LIB CAM.

Due to their different foci, both the HTL/THP and LCA (HTox) approaches can be seen as complementary, allowing fast hazard screening of potential CAM precursors under different perspectives. However, for interpreting the results, it is crucial to consider the uncertainties intrinsic to these methods, which partially originate from the early-stage CAM production pathways (low TRL) and the related lack of data for precursors and synthesis routes. However, despite these uncertainties, the methods presented in this work are applicable on high, but also even at very low TRL levels and with data available on laboratory scale, and therefore can support early-stage material choices considering upcoming hazard labeling requirements. To the best of our knowledge, this approach has not been described in detail in the literature or the Battery Regulation.[2,3]

Cell developers can apply the named methods for their specific lab scale using all the available data. This is also appli-

 

cable for battery cell producers to screen their product portfolio considering mandatory reporting on hazardous substances. Using and combining these different methods can lower the risk of making the wrong decision in uncertain situations and to avoid overlooking problematic material choices. The first method, the HTL, is highly qualitative but provides a quick overview of potential hazards with a simple visualization approach. THP represent an extension of the HTL given that they incorporate quantity thresholds (LT – lower tier), as defined in the Seveso III Directive.[23] This allows potential hazards to be quantified for different CAM, and thus enables direct comparison.

Under both approaches, all SIB pose hazards, although with substantial differences between individual CAM. In the case of oxidic CAM, NMC (the LIB reference) obtains very high hazard scores, which are mainly due to cobalt and nickel sulfate. In comparison, SIB show lower scores, with the only exceptions of SIB variants that also contain a high amount of Ni. In the case of the polyanionic CAM, the LFP reference achieves a significantly lower hazard score than its oxidic Li-based counterpart. However, here, most SIB CAM obtain lower scores than the LIB reference (LFP), with the only exceptions also being vanadium-containing alternatives. Here, the proposed methods allow the comparison of different suitable precursors for CAM synthesis, and therefore can provide decision aid for precursor selection, as demonstrated for different vanadium-based precursors for $Na_3V_2(PO_4)_3$.

It is hardly possible to directly compare the results of HTL and THP with that of the third, life-cycle based approach (HTox), given that they are based on different scales, modelling methods and system boundaries. Nevertheless, their comparison is helpful to provide an additional, complementary perspective, which also allows the identification of potential hazard hotspots for substances that have a low or no substance classification. Interestingly, and despite the very different perspectives, in the case of the oxidic SIB variants, the LCA results for HTox provide a comparable picture as the THP. This is true to a certain degree for the polyanionic SIB CAM alternatives, where for all methods, the vanadium-containing CAM have the highest potential impacts. Here, $V_2O_5$ has a high contribution to the results, resulting in higher impacts than substance alternatives. This is also the case for the qualitative comparison and composite indicator, where named CAM alternatives are ranked the last with corresponding high hazard and toxicity risks.

In the case of both quantitative methods (THP and HTox), when comparing the results on a mass basis (per kg of CAM) and a specific capacity basis (per kW h of energy capacity), it becomes apparent that the energy density is one of the most important factors for the hazard and toxicity screening, being a key determinant for the material demand. This, naturally, is independent of the applied method.

As stated before, the HTL and THP may be prone to uncertainty in low TRL, given that some rather new chemicals may not be yet classified in the ECHA database (or any other database). The same is true for the LCA, which is based on the ecoinvent database, and therefore the availability of precursor materials within. Finally, the current screening is limited to CAM, and upon reaching a higher TRL, it will be recommended to go a step further and evaluate in detail an entire cell of selected SIBs including different electrolytes, separators, and anodes to provide a more comprehensive picture of potential impacts and hazards, which is consistent with the recommendations by the Battery Passport. Subsequently, this will also tackle PFAS contained in the electrode binders and provide a different picture. Considered this, the presented methods and exploratory results can be of added value for any cell developer or manufacturer that must comply with current regulations.

## Conflicts of interest

There are no conflicts to declare.

## Acknowledgements

This work contributes to the research performed within the Helmholtz Association project “Energy System 2050 “and at CELEST (Center for Electrochemical Energy Storage Ulm-Karlsruhe) which is funded by the German Research Foundation (DFG) under Project ID 390874152 (POLiS Cluster of Excellence). The publication is part of the grant RYC2022-037773-I, financed by the Spanish Ministry of Science and Innovation (MCIN/AEI/10.13039/501100011033) and by the European Social Fund ESF+.

## References

1 BloombergNEF, 1H 2023 Energy Storage Market Outlook, 2023, Available from: **https://about.bnef.com/blog/1h-2023-energy-storage-market-outlook/**.
2 European Union, REGULATION (EU) 2023/1542 OF THE EUROPEAN PARLIAMENT AND OF THE COUNCIL of 12 July 2023 concerning batteries and waste batteries, amending Directive 2008/98/EC and Regulation (EU) 2019/1020 and repealing Directive 2006/66/EC, 2023Jul [cited 2023 Oct 17], Report No.: EU, Available from: **https://eur-lex.europa.eu/legal-content/EN/TXT/PDF/?uri=CELEX:32023R1542**.
3 D. Aschermayr, S. Kadner, L. Risch, *et al.*, Battery Passport Content Guidance - Achieving compliance with the EU Battery Regulation and increasing sustainability and circularity, Federal Ministry for Economic Affairs and Climate Action, 2023Apr, Available from: **https://thebatterypass.eu/assets/images/content-guidance/pdf/2023_Battery_Passport_Content_Guidance.pdf**.
4 European Commission, COM(2020) 667 final - Chemicals Strategy for Sustainability Towards a Toxic-Free Environment, Brüssels, 2020Oct, Available from: **https://environment.ec.europa.eu/strategy/chemicals-strategy_en**.

5 OECD, Guidance on Key Considerations for the Identification and Selection of Safer Chemical Alternative, OECD Series on Risk Management, 2021;No 60, Available from: https://www.oecd.org/chemicalsafety/risk-management/substitution-of-hazardous-chemicals/.
6 M. K. M. Lane, H. E. Rudel, J. A. Wilson, H. C. Erythropel, A. Backhaus, E. B. Gilcher, *et al.*, Green chemistry as just chemistry, *Nat. Sustain.*, 2023, **6**(5), 502–512.
7 J. F. Peters, M. Baumann, J. R. Binder and M. Weil, On the environmental competitiveness of sodium-ion batteries under a full life cycle perspective – a cell-chemistry specific modelling approach, *Sustainable Energy Fuels*, 2021, **5**, 6414–6429.
8 M. Baumann, M. Häringer, M. Schmidt, L. Schneider, J. F. Peters, W. Bauer, *et al.*, Prospective Sustainability Screening of Sodium–Ion Battery Cathode Materials, *Adv. Energy Mater.*, 2022, 2202636.
9 CIC energigune, The sodium-ion battery boom: The perfect (and sustainable) complement to lithium-ion batteries, Media Center, 2022, Available from: https://cicenergigune.com/en/blog/sodium-battery-perfect-sustainable-complement-lithium-batteries.
10 TIAMAT, 2021, Available from: https://www.tiamat-energy.com/.
11 CATL, CATL Unveils Its Latest Breakthrough Technology by Releasing Its First Generation of Sodium-ion Batteries, 2021, Available from: https://www.catl.com/en/news/665.html.
12 Faradion, Farardion, Technology Benefits, 2021, Available from: https://www.faradion.co.uk/technology-benefits/sustainable-technology/.
13 HiNa, HiNa Battery, HiNa Battery, 2023, Available from: https://www.hinabattery.com/en/.
14 H. Liu, M. Baumann, X. Dou, J. Klemens, L. Schneider, A. K. Wurba, *et al.*, Tracing the technology development and trends of hard carbon anode materials - A market and patent analysis, *J. Energy Storage*, 2022, **56**, 105964.
15 Q. Liu, Z. Hu, W. Li, C. Zou, H. Jin, S. Wang, *et al.*, Sodium transition metal oxides: the preferred cathode choice for future sodium-ion batteries?, *Energy Environ. Sci.*, 2021, **14**(1), 158–179.
16 T. Liu, Y. Zhang, Z. Jiang, X. Zeng, J. Ji, Z. Li, *et al.*, Exploring competitive features of stationary sodium ion batteries for electrochemical energy storage, *Energy Environ. Sci.*, 2019, **12**(5), 1512–1533.
17 EU 2006 Regulation (EC) No 1907/2006 of the European Parliament and of the Council of 18 December 2006 concerning the Registration, Evaluation, Authorisation and Restriction of Chemicals (REACH), establishing a European Chemicals Agency, amending Directive 1999/45/EC and repealing Council Regulation (EEC) No 793/93 and Commission Regulation (EC) No 1488/94 as well as Council Directive 76/769/EEC and Commission Directives 91/155/EEC, 93 vol L 396, Brussels, Belgium: European Parliament, 2006, Available from: https://eur-lex.europa.eu/legal-content/en/ALL/?uri=CELEX%3A32006R1907.
18 EU, Directive 2012/18/EU of the European Parliament and of the Council of 4 July 2012 on the control of major-accident hazards involving dangerous substances, amending and subsequently repealing Council Directive 96/82/EC, Brüssel, 2012, Available from: https://eur-lex.europa.eu/legal-content/EN/TXT/?uri=celex%3A32012L0018.
19 H. Stahl, D. Bauknecht, A. Hermann, W. Jenseit, A. Köhler, C. Merz, *et al.*, Ableitung von Recycling- und Umweltanforderungen und Strategien zur Vermeidung von ersorgungsrisiken bei innovativen Energiespeichern, Dessau-Roßlau: Umweltbundesamt, 2015Aug. Report No.: UBA-FB 002218, Available from: https://www.umweltbundesamt.de/sites/default/files/medien/378/publikationen/texte_07_2016_ableitung_von_recycling-und_umweltanforderungen.pdf.
20 G. Rodriguez-Garcia, J. Braun, J. Peters and M. Weil, Hazard statements: looking for alternatives to toxicity evaluation using LCA, *Matér. Tech.*, 2017, **105**(5–6), 517.
21 J. A. Jeevarajan, T. Joshi, M. Parhizi, T. Rauhala and D. Juarez-Robles, Battery Hazards for Large Energy Storage Systems, *ACS Energy Lett.*, 2022, **7**(8), 2725–2733.
22 European Commission (EC), Recommendation on the use of the Environmental Footprint methods to measure and communicate the life cycle environmental performance of products and organisations, Brussels, 2021, Report No.: C(2021) 9332 final, Available from: https://environment.ec.europa.eu/system/files/2021-12/Commission%20Recommendation%20on%20the%20use%20of%20the%20Environmental%20Footprint%20methods_0.pdf.
23 EC, Regulation (EC) No 1272/2008 of the European Parliament and of the Council of 16 December 2008 on classification, labelling and packaging of substances and mixtures, amending and repealing Directives 67/548/EEC and 1999/45/EC, and amending Regulation (EC) No 1907/2006, Dec 16, 2008.
24 M. Quant, O. Willstrand, T. Mallin and J. Hynynen, Ecotoxicity Evaluation of Fire-Extinguishing Water from Large-Scale Battery and Battery Electric Vehicle Fire Tests, *Environ. Sci. Technol.*, 2023, **57**(12), 4821–4830.
25 C. R. Hung, L. A. Ellingsen and G. Majeau-Bettez, LiSET: A Framework for Early–Stage Life Cycle Screening of Emerging Technologies, *J. Ind. Ecol.*, 2020, **24**(1), 26–37.
26 F. Gschwind, G. Rodriguez-Garcia, D. J. S. Sandbeck, A. Gross, M. Weil, M. Fichtner, *et al.*, Fluoride ion batteries: Theoretical performance, safety, toxicity, and a combinatorial screening of new electrodes, *J. Fluorine Chem.*, 2016, **182**, 76–90.
27 J. Peters, D. Buchholz, S. Passerini and M. Weil, Life cycle assessment of sodium-ion batteries, *Energy Environ. Sci.*, 2016, **9**(5), 1744–1751.
28 P. A. Nelson, K. G. Gallagher, I. Bloom and D. W. Dees, *Modeling the Performance and Cost of Lithium-Ion Batteries for Electric-Drive Vehicles/BatPaC model*, Argonne National laboratory, Chicago, 2011.
29 I. Rey, M. Iturrondobeitia, O. Akizu-Gardoki, R. Minguez and E. Lizundia, Environmental Impact Assessment of $Na_3V_2$

 

$(PO_4)_3$ Cathode Production for Sodium–Ion Batteries, *Adv. Energy Sustainability Res.*, 2022, **3**(8), 2200049.

30 R. Hischier, N. H. Kwon, J. Brog and K. M. Fromm, Early–Stage Sustainability Evaluation of Nanoscale Cathode Materials for Lithium Ion Batteries, *ChemSusChem*, 2018, **11**(13), 2068–2076.

31 L. Ellingsen, A. Holland, J. F. Drillet, W. Peters, M. Eckert, C. Concepcion, *et al.*, Environmental Screening of Electrode Materials for a Rechargeable Aluminum Battery with an AlCl3/EMIMCl Electrolyte, *Materials*, 2018, **11**(6), 936.

32 F. Gschwind, H. Euchner and G. Rodriguez-Garcia, Chloride Ion Battery Review: Theoretical Calculations, State of the Art, Safety, Toxicity, and an Outlook towards Future Developments, *Eur. J. Inorg. Chem.*, 2017, **2017**(21), 2784–2799.

33 H. He, S. Tian, C. Glaubensklee, B. Tarroja, S. Samuelsen, O. A. Ogunseitan, *et al.*, Advancing chemical hazard assessment with decision analysis: A case study on lithium-ion and redox flow batteries used for energy storage, *J. Hazard. Mater.*, 2022, **437**, 129301.

34 European Commission, Joint Research Centre, Safe and sustainable by design chemicals and materials: framework for the definition of criteria and evaluation procedure for chemicals and materials, LU: Publications Office, 2022 [cited 2024 Apr 1], Available from: **https://data.europa.eu/**, DOI: **10.2760/487955**.

35 ECHA, Per- and polyfluoroalkyl substances (PFAS), 2023, Available from: **https://echa.europa.eu/hot-topics/perfluoroalkyl-chemicals-pfas**.

36 X. Pu, H. Wang, T. Yuan, S. Cao, S. Liu, L. Xu, *et al.*, Na4Fe3(PO4)2P2O7/C nanospheres as low-cost, high-performance cathode material for sodium-ion batteries, *Energy Storage Mater.*, 2019, **22**, 330–336.

37 T. Yuan, Y. Wang, J. Zhang, X. Pu, X. Ai, Z. Chen, *et al.*, 3D graphene decorated Na4Fe3(PO4)2(P2O7) microspheres as low-cost and high-performance cathode materials for sodium-ion batteries, *Nano Energy*, 2019, **56**, 160–168.

38 A. Zhao, T. Yuan, P. Li, C. Liu, H. Cong, X. Pu, *et al.*, A novel Fe-defect induced pure-phase Na4Fe2.91(PO4)2P2O7 cathode material with high capacity and ultra-long lifetime for low-cost sodium-ion batteries, *Nano Energy*, 2022, **91**, 106680.

39 R. Sun and Y. You, Prussian White Cathode Materials for All-Climate Sodium-Ion Batteries, *ACS Appl. Mater. Interfaces*, 2023, **15**(38), 44599–44606.

40 G. Patnaik, I. Escher, G. A. Ferrero and P. Adelhelm, Electrochemical Study of Prussian White Cathodes with Glymes – Pathway to Graphite–Based Sodium–Ion Battery Full Cells, *Batteries Supercaps*, 2022, **5**(7), e202200043.

41 J. H. Mugumya, M. L. Rasche, R. F. Rafferty, A. Patel, S. Mallick, M. Mou, *et al.*, Synthesis and Theoretical Modeling of Suitable Co-precipitation Conditions for Producing NMC111 Cathode Material for Lithium-Ion Batteries, *Energy Fuels*, 2022, **36**(19), 12261–12270.

42 D. Gastol, J. Marshall, E. Cooper, C. Mitchell, D. Burnett, T. Song, *et al.*, Reclaimed and Up–Cycled Cathodes for Lithium–Ion Batteries, *Global Chall.*, 2022, **6**(12), 2200046.

43 C. Nan, J. Lu, C. Chen, Q. Peng and Y. Li, Solvothermal synthesis of lithium iron phosphate nanoplates, *J. Mater. Chem.*, 2011, **21**(27), 9994.

44 J. Kang, S. Baek, V. Mathew, J. Gim, J. Song, H. Park, *et al.*, High rate performance of a Na3V2(PO4)3/C cathode prepared by pyro-synthesis for sodium-ion batteries, *J. Mater. Chem.*, 2012, **22**(39), 20857.

45 C. Zhao, L. Liu, Y. Lu, M. Wagemaker, L. Chen and Y. Hu, Revealing an Interconnected Interfacial Layer in Solid–State Polymer Sodium Batteries, *Angew. Chem., Int. Ed.*, 2019, **58**(47), 17026–17032.

46 M. F. Rosle, N. Najmi, M. I. Ishak, M. Mohamad Saman and A. H. Hashim, Calcination effect on particle morphologies and electrochemical performances of Na3V2(PO4)3/C composites as cathode for sodium-ion batteries, *Mater. Today: Proc.*, 2019, **16**, 1856–1863.

47 X. Liu, X. Jiang, F. Zhong, X. Feng, W. Chen, X. Ai, *et al.*, High-Safety Symmetric Sodium-Ion Batteries Based on Nonflammable Phosphate Electrolyte and Double $Na_3V_2(PO_4)_3$ Electrodes, *ACS Appl. Mater. Interfaces*, 2019, **11**(31), 27833–27838.

48 T. Akçay, M. Häringer, K. Pfeifer, J. Anhalt, J. R. Binder, S. Dsoke, *et al.*, $Na_3V_2(PO_4)_3$ —A Highly Promising Anode and Cathode Material for Sodium-Ion Batteries, *ACS Appl. Energy Mater.*, 2021, **4**(11), 12688–12695.

49 J. Billaud, G. Singh, A. R. Armstrong, E. Gonzalo, V. Roddatis, M. Armand, *et al.*, $Na_{0.67}Mn_{1-x}Mg_xO_2$ ($0 \leq x \leq 0.2$): a high capacity cathode for sodium-ion batteries, *Energy Envorin. Sci.*, 2014, **7**(4), 1387–1391.

50 J. Song, L. Wang, Y. Lu, J. Liu, B. Guo, P. Xiao, *et al.*, Removal of Interstitial $H_2O$ in Hexacyanometallates for a Superior Cathode of a Sodium-Ion Battery, *J. Am. Chem. Soc.*, 2015, **137**(7), 2658–2664.

51 Y. You, X. L. Wu, Y. X. Yin and Y. G. Guo, High-quality Prussian blue crystals as superior cathode materials for room-temperature sodium-ion batteries, *Energy Environ. Sci.*, 2014, **7**(5), 1643–1647.

52 D. Yang, J. Xu, X. Z. Liao, H. Wang, Y. S. He and Z. F. Ma, Prussian blue without coordinated water as a superior cathode for sodium-ion batteries, *Chem. Commun.*, 2015, **51**(38), 8181–8184.

53 X. Jiang, F. Hu and J. Zhang, Sodium-deficient O3–$Na_{0.9}Mn_{0.4}Fe_{0.5}Ti_{0.1}O_2$ as a cathode material for sodium-ion batteries, *RSC Adv.*, 2016, **6**(105), 103238–103241.

54 J. Kim, D. H. Seo, H. Kim, I. Park, J. K. Yoo, S. K. Jung, *et al.*, Unexpected discovery of low-cost maricite $NaFePO_4$ as a high-performance electrode for Na-ion batteries, *Energy Environ. Sci.*, 2015, **8**(2), 540–545.

55 H. Kim, G. Yoon, I. Park, J. Hong, K. Y. Park, J. Kim, *et al.*, Highly Stable Iron- and Manganese-Based Cathodes for Long-Lasting Sodium Rechargeable Batteries, *Chem. Mater.*, 2016, **28**(20), 7241–7249.

56 W. Guan, B. Pan, P. Zhou, J. Mi, D. Zhang, J. Xu, *et al.*, A High Capacity, Good Safety and Low Cost $Na_2FeSiO_4$-Based Cathode for Rechargeable Sodium-Ion Battery, *ACS Appl. Mater. Interfaces*, 2017, **9**(27), 22369–22377.

57 M. Law, V. Ramar and P. Balaya, Na2MnSiO4 as an attractive high capacity cathode material for sodium-ion battery, *J. Power Sources*, 2017, **359**, 277–284.
58 X. Lin, X. Hou, X. Wu, S. Wang, M. Gao and Y. Yang, Exploiting $Na_2MnPO_4F$ as a high-capacity and well-reversible cathode material for Na-ion batteries, *RSC Adv.*, 2014, **4**(77), 40985–40993.
59 S. W. Kim, D. H. Seo, H. Kim, K. Y. Park and K. Kang, A comparative study on Na2MnPO4F and Li2MnPO4F for rechargeable battery cathodes, *Phys. Chem. Chem. Phys.*, 2012, **14**(10), 3299.
60 D. Liu and G. T. R. Palmore, Synthesis, Crystal Structure, and Electrochemical Properties of Alluaudite $Na_{1.702}Fe_3(PO_4)_3$ as a Sodium-Ion Battery Cathode, *ACS Sustainable Chem. Eng.*, 2017, **5**(7), 5766–5771.
61 N. Yabuuchi, M. Kajiyama, J. Iwatate, H. Nishikawa, S. Hitomi, R. Okuyama, *et al.*, P2-type Nax[Fe1/2Mn1/2]O2 made from earth-abundant elements for rechargeable Na batteries, *Nat. Mater.*, 2012, **11**(6), 512–517.
62 D. Kim, E. Lee, M. Slater, W. Lu, S. Rood and C. S. Johnson, Layered Na[Ni1/3Fe1/3Mn1/3]O2 cathodes for Na-ion battery application, *Electrochem. Commun.*, 2012, **18**, 66–69.
63 I. Hasa, S. Passerini and J. Hassoun, A rechargeable sodium-ion battery using a nanostructured Sb–C anode and P2-type layered $Na_{0.6}Ni_{0.22}Fe_{0.11}Mn_{0.66}O_2$ cathode, *RSC Adv.*, 2015, **5**(60), 48928–48934.
64 P. F. Wang, Y. You, Y. X. Yin and Y. G. Guo, An O3-type $NaNi_{0.5}Mn_{0.5}O_2$ cathode for sodium-ion batteries with improved rate performance and cycling stability, *J. Mater. Chem. A*, 2016, **4**(45), 17660–17664.
65 X. Ma, H. Chen and G. Ceder, Electrochemical Properties of Monoclinic $NaMnO_2$, *J. Electrochem. Soc.*, 2011, **158**(12), A1307.
66 N. Yabuuchi, M. Yano, H. Yoshida, S. Kuze and S. Komaba, Synthesis and Electrode Performance of O3-Type $NaFeO_2$-$NaNi_{1/2}Mn_{1/2}O_2$ Solid Solution for Rechargeable Sodium Batteries, *J. Electrochem. Soc.*, 2013, **160**(5), A3131–A3137.
67 E. Talaie, V. Duffort, H. L. Smith, B. Fultz and L. F. Nazar, Structure of the high voltage phase of layered P2-$Na_{2/3-z}[Mn_{1/2}Fe_{1/2}]O_2$ and the positive effect of Ni substitution on its stability, *Energy Environ. Sci.*, 2015, **8**(8), 2512–2523.
68 I. Hasa, S. Passerini and J. Hassoun, Toward high energy density cathode materials for sodium-ion batteries: investigating the beneficial effect of aluminum doping on the P2-type structure, *J. Mater. Chem. A*, 2017, **5**(9), 4467–4477.
69 P. Ramesh Kumar, A. Kheireddine, U. Nisar, R. A. Shakoor, R. Essehli, R. Amin, *et al.*, Na4MnV(PO4)3-rGO as Advanced cathode for aqueous and non-aqueous sodium ion batteries, *J. Power Sources*, 2019, **429**, 149–155.
70 T. Zhu, P. Hu, C. Cai, Z. Liu, G. Hu, Q. Kuang, *et al.*, Dual carbon decorated Na3MnTi(PO4)3: A high-energy-density cathode material for sodium-ion batteries, *Nano Energy*, 2020, **70**, 104548.
71 H. Gao, I. D. Seymour, S. Xin, L. Xue, G. Henkelman and J. B. Goodenough, $Na_3MnZr(PO_4)_3$ : A High-Voltage Cathode for Sodium Batteries, *J. Am. Chem. Soc.*, 2018, **140**(51), 18192–18199.
72 United Nations Economic Commission for Europe, Globally Harmonized System of Classification and Labelling of Chemicals (GHS), About the GHS, 2023, Available from: **https://unece.org/about-ghs**.
73 ECHA, European Chemicals Agency, Search for chemicals, 2022, Available from: **https://echa.europa.eu/search-for-chemicals?p_p_id=disssimplesearch_WAR_disssearchportlet&p_p_lifecycle=0&_disssimplesearch_WAR_disssearchportlet_searchOccurred=true&_disssimplesearch_WAR_disssearchportlet_sessionCriteriaId=dissSimpleSearchSessionParam101401642518674625**.
74 ECHA, SCIP, ECHA European Chemicals Agency, 2023, Available from: **https://echa.europa.eu/scip**.
75 ECHA, Table of harmonised entries in Annex VI to CLP, 2023, Available from: **https://echa.europa.eu/en/information-on-chemicals/annex-vi-to-clp**.
76 REACH Compliance GmbH, Gefahrenpiktogramme zum Download, 2022, Available from: **https://www.reach-compliance.ch/ghsclp/index.html**.
77 S. Sala, F. Biganzoli, E. S. Mengual and E. Saouter, Toxicity impacts in the environmental footprint method: calculation principles, *Int. J. Life Cycle Assess.*, 2022, **27**(4), 587–602.
78 R. K. Rosenbaum, T. M. Bachmann, L. S. Gold, M. A. J. Huijbregts, O. Jolliet, R. Juraske, *et al.*, USEtox—the UNEP-SETAC toxicity model: recommended characterisation factors for human toxicity and freshwater ecotoxicity in life cycle impact assessment, *Int. J. Life Cycle Assess.*, 2008, **13**(7), 532–546.
79 Swiss Center for Life Cycle Inventories, Ecoinvent centre, Zürich, CH: Swiss Center for Life Cycle Inventories, 2012[cited 2012 Apr 20], Available from: **https://www.ecoinvent.ch/**.
80 S. Weber, J. F. Peters, M. Baumann and M. Weil, Life Cycle Assessment of a Vanadium Redox Flow Battery, *Environ. Sci. Technol.*, 2018, **52**(18), 10864–10873.
81 ECHA, Harmonised classification and labelling (CLH), 2023[cited 2023 Aug 2], Available from: **https://echa.europa.eu/regulations/clp/harmonised-classification-and-labelling**.
82 National Library of Medicine, Sodium Ferrocynaide, 2023, Available from: **https://pubchem.ncbi.nlm.nih.gov/compound/Sodium-ferrocyanide**.
83 M. J. Baumann, J. F. Peters, M. Weil and A. Grunwald, CO2 footprint and life cycle costs of electrochemical energy storage for stationary grid applications, *Energy Technol.*, 2016, **5**, 1071–1083, [cited 2017 Jan 17].
84 A. Rensmo, E. K. Savvidou, I. T. Cousins, X. Hu, S. Schellenberger and J. P. Benskin, Lithium-ion battery recycling: a source of per- and polyfluoroalkyl substances (PFAS) to the environment?, *Environ. Sci.: Processes Impacts*, 2023, **25**(6), 1015–1030.